Chemical fingerprints and microbial biomineralization of fish muscle tissues from the Late Cretaceous Múzquiz Lagerstätte, Mexico

Francisco Riquelme[1, *], Jesús Alvarado-Ortega[2], José Luis Ruvalcaba-Sil[1], Manuel Aguilar-Franco[1], and Héctor Porras-Múzquiz[3]

[1] Instituto de Física, Universidad Nacional Autónoma de México, A. P. 20-364, México, D.F., Mexico.
[2] Instituto de Geología, Universidad Nacional Autónoma de México, Circuito de la Investigación S/N, Ciudad Universitaria, Coyoacán, 04510 México, D.F., Mexico.
[3] Museo Histórico de Múzquiz, Hidalgo 205, Centro, 26340 Múzquiz, Coahuila, Mexico.
** riquelme.fc@gmail.com*

ABSTRACT

Fossil fish specimens from the Múzquiz Lagerstätte (Late Cretaceous) of northern México have been analysed using UV light-induced visible fluorescence microscopy, Particle-induced X-ray Emission (PIXE), X-Ray Diffraction (XRD), and Scanning Electron Microscopy (SEM). Specimens examined with UV light microscopy show tightly packed trunk muscle tissues and digestive tract contents, as well as a color gradient from pink to orange to brown associated with the chemical state of the muscle tissues. PIXE analysis shows a 0.346 P/Ca ratio in muscle tissues, as well as a phosphorus increase by a factor of more than four compared to surrounding sediment. Quantitative XRD analysis shows that cryptocrystalline flourapatite (FAP) is the predominant mineral phase and calcite is complementary in the muscle tissues. Nucleation of FAP and calcite may have occurred simultaneously with organic decay, forming adhesive pellets in the soft watery carbonate mud, and caused immobilization of the carcasses. Electron microscope scans show muscle tissues preserved with cellular and subcellular features as well as digestive tract contents with calcareous nanoplankton. Fossil biofilms with bacteria have also been exceptionally preserved as intact cells, casts and molds. This cell-specific, rapid mineralization can be explained by a crystal seed process, which is discussed here.

Key words: fossil fish, exceptional preservation, PIXE spectrometry, biomineralization, Cretaceous, Múzquiz, Mexico.

RESUMEN

Ejemplares de peces del Lagerstätte de Múzquiz (Cretácico Tardío) del norte de México han sido analizados usando microscopía de fluorescencia visible inducida por luz UV, Emisión de Rayos X Inducida por Partículas (PIXE), Difracción de Rayos X (DRX), y Micoscopía Electrónica de Barrido (MEB). Los peces examinados preliminarmente por microscopía de luz UV muestran tejidos musculares del torso y contenido del tracto digestivo, así como un gradiente de color de rosa-anaranjado-parduzco asociado con el estado químico de los tejidos musculares. El análisis por medio de PIXE muestra una relación de P/Ca de 0.346 en tejido muscular, así como un incremento en el contenido de fósforo

por un factor de más de cuatro en comparación con los sedimentos. Análisis cuantitativos de DRX muestran que fluourapatita (FAP) criptocristalina es la fase mineral predominante, mientras calcita es complementaria en los tejidos musculares. La nucleación de FAP y calcita pudo ocurrir simultáneamente a la degradación orgánica y causó la inmovilización de los cadáveres formando pellets adhesivos en un lodo de carbonatos blando y acuoso. Análisis de microscopía electrónica muestran tejidos musculares con rasgos celulares y subcelulares, así como contenido del tracto digestivo con nanoplancton calcáreo. Biopelículas fósiles con bacterias han sido también preservadas como células intactas, costras y moldes. Esta rápida mineralización, celular-específica, puede explicarse por el proceso de semilla cristalina, el cual es discutido aquí.

Palabras clave: peces fósiles, preservación excepcional, espectrometría PIXE, biomineralización, Cretácico, Múzquiz, México.

INTRODUCTION

A diverse fossil assemblage has been collected systematically over the past ten years from a series of sites in northern Coahuila, Mexico, which are referred to here as the Múzquiz Lagerstätte type localities (late Turonian - early Coniacian; Figure 1). These sites yield exceptional fossil preservation in fishes, including soft parts and tissues, as shown for example by Seilacher *et al.* (1985), Allison (1988), and Botjer *et al.* (2002). The fossil assemblage includes marine invertebrates and vertebrates, such as inoceramid bivalves, ammonoids, crustaceans, reptiles, actinopterygians, and chondrichthyans (Blanco-Piñón and Alvarado-Ortega, 2005; Buchy *et al.*, 2005; Nyborg *et al.*, 2005; Stinnesbeck *et al.*, 2005; Frey *et al.*, 2006; Alvarado-Ortega *et al.*, 2006; Vega *et al.*, 2007; Alvarado-Ortega and Porras-Múzquiz, 2009). Typically, the fishes are preserved three-dimensionally and are well-articulated, exhibiting preservation of soft tissue anatomy, including parts of the digestive tract and muscle mass, with exquisite detail, and evidence of microbially mediated organic decay (Alvarado-Ortega and Porras-Múzquiz, 2009, Riquelme *et al.*, 2010).

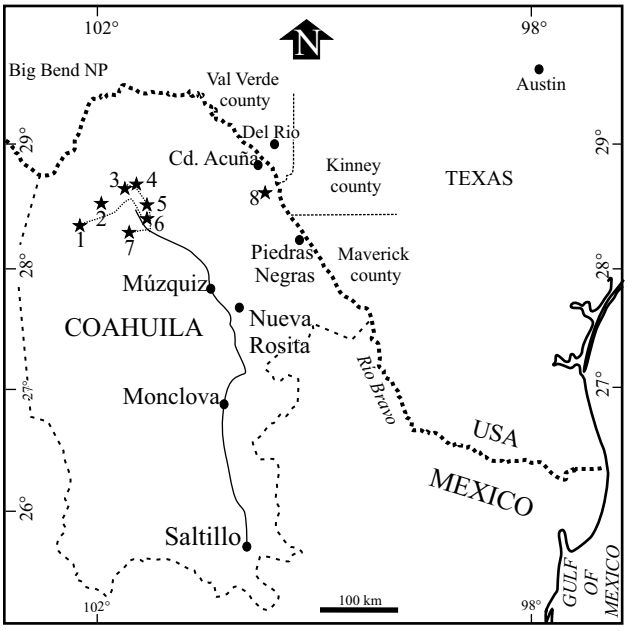

Figure 1. Location of Múzquiz Lagerstätte type localities, in northern Coahuila. 1: Piedritas, 2: Jaboncillos, 3: La Mula, 4: Venustiano Carranza, 5: Los Temporales, 6: El Rosario, 7: El Pilote, 8: Palestina.

The fossils occur in limestone-marl alternations, a particular type of fine-grained calcareous rythmite (Figure 2). The two conspicuous attributes of the rythmites is their cyclical nature with apparently different diagenetic histories, and the occurrence of well-preserved fossils on the laminar interfaces. Little is known about the genesis of these rythmites and the fossilization process involved in preservation of the Múzquiz biota, for which there are no published taphomic studies. Preliminary interpretations regarding the depositional environment of the Múzquiz Lagerstätte are found in paleontological and biostratigraphic studies of a number of small quarries within an area of approximately 170 km^2, such as El Rosario (Stinnesbeck *et al.*, 2005); La Mula (Blanco-Piñón and Alvarado-Ortega, 2005); Venustiano Carranza, Los Temporales, El Pilote (Alvarado-Ortega *et al.*, 2006; Vega *et al.*, 2007; Alvarado-Ortega and Porras-Múzquiz, 2009), Jaboncillos, and Piedritas (Alvarado-Ortega and Riquelme, 2010; pers. obs.). The depositional environment associated with these sediments has been tentatively interpreted as an open marine shelf with hostile, oxygen-deficient, bottom waters (*e.g.*, Blanco-Piñón and Alvarado-Ortega, 2005; Nyborg *et al.*, 2005; Stinnesbeck *et al.*, 2005, Alvarado-Ortega *et al*, 2006; Vega *et al.*, 2007).

The aim of the present work is to provide microscopic and biogeochemical data on the exceptionally preserved fossils using a combination of high-resolution scanning electron microscopy (SEM), UV light microscopy, X-ray diffraction (XRD), and particle induced X-ray emission spectrometry (PIXE). This work represents a first approach to understanding the fossilization process that occurred in the Múzquiz Lagerstätte through a more detailed documentation of its biogeochemical pathways.

Múzquiz Lagerstätte type localities

The outcrops of Upper Cretaceous marine strata exposed near the municipality of Múzquiz and in the surrounding area of northern Coahuila provide some of the most spectacular fossil-rich deposits in Mexico (Figure 1). These deposits accumulated in diverse marine environments that were related to the Western Interior Seaway, which extended from the northern Tethys Ocean into North America (Goldhammer, 1999; Goldhammer and Johnson, 2001), and are usually regarded as correlative with the Austin Chalk and Eagle Ford Groups exposed in northern Coahuila and Texas (Sohl *et al.*, 1991; Eguiluz de Antuñano, 2001). These strata consist mainly of chalk, limestone, and organic-rich mudstone deposited during the peak transgression of the Late Cretaceous epeiric sea in North America (Smith, 1981; Sohl *et al.*, 1991; Young, 1985; Young, 1986).

The Eagle Ford sequence includes black shale, yellowish-gray limestone, and interbedded marlstone dated as Cenomanian-Turonian in age (Myers, 2010). The Eagle Ford strata conformably overlie the Buda Limestone and are conformably overlain by a sequence of recrystallized limestone, chalk, and marl of Coniacian-Santonian age correlative with the Austin Chalk (Dravis, 1980; Larson *et al.,* 1991).

The stratigraphic nomenclature changes in southwestern Texas from Eagle Ford/Austin to Boquillas (Lock and Peschier, 2006); for example, in the Big Bend region (Figure 1), where the overlying lower unit of the Austin Chalk is included as the San Vicente Formation within the Boquillas Group (*e.g.*, Freeman, 1961, Donovan and Staerker, 2010, Lock *et al.*, 2010). The Eagle Ford and Austin Chalk terms are generally used for correlative strata exposed on the central and eastern Texas coastal plain; however, in Coahuila it is difficult to differentiate the Eagle Ford from other units or to recognize its members. The strata exposed in Coahuila span an age range different from the Boquillas, San Vicente, or Austin Chalk formations (*e.g.*, Eguiluz de Antuñano, 2001; SGM, 2008a, 2008b). In the present paper, the term Eagle Ford (Boquillas) is used.

The Múzquiz Lagerstätte occurs in a series of restricted outcrops within a repetitive sequence of fine-grained calcareous rythmites. The lithology consists of platy limestone alternating with impure chalk and marlstone with earthy texture. Most of the argillaceous material is found as stratified millimeter-thick layers of volcaniclastic bentonitic clay. Some exposures also exhibit irregular lenses and flaky nodules of iron hydroxides, as well as minor thin layers of indurated non-fissile siltstone and grayish-black, thinly laminated calcareous shale.

Two localities are highlighted here due to the remarkable preservation of fish specimens: El Pilote and Palestina quarries (Alvarado-Ortega *et al.*, 2006; Vega *et al.*, 2007; Riquelme *et al.*, 2010). Although the two sites show differences in their taphonomic features and variations in lithology, they exhibit comparable preservation in fossil fishes, including three-dimensionally preserved morphology, articulated skeletons, muscle tissue remains, and evidence of restricted organic decay.

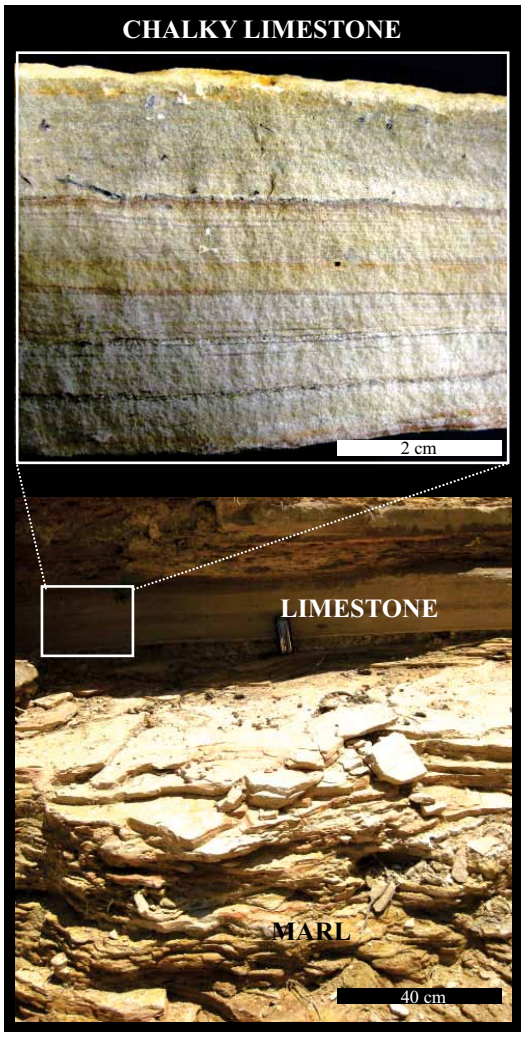

Figure 2. Limestone-marl rythmites of the Múzquiz Lagerstätte type locality (below), and a detailed view of the typical laminated chalky limestone (above). Palestina quarry.

Palestina quarry

Palestina quarry is located 290 km northeast of Múzquiz, near the town of Acuña, at latitude 29°11'57'' N, longitude 100°53'20'' W (Figure 1). The average altitude here is 300 m above sea level, in an area mapped as the Coniacian-Santonian Austin Chalk Formation (SGM, 2008a). Palestina is a very restricted outcrop composed predominantly of creamy-yellow, platy, chalky limestone intercalated with marl (Figure 2). Minor indurated non-fissile siltstone and unconsolidated iron oxides, with volcaniclastic bentonitic clay, is periodically exposed as 3 to 5 cm thick layers in the upper beds. Neither the base nor the top of the section are exposed.

The upper fossiliferous chalky beds are finely crystalline, and frequently contain invertebrates such as inoceramid bivalves and gastropods with well-preserved calcareous shells. Microscopic analyses also reveal that the content of foraminifera, calcareous filamentous algae, and calcareous nanoplankton is significantly greater in these layers, with coccoliths being very abundant. Vertebrate fossils are absent in the upper layers, whereas the chalky limestones in the lower beds yield abundant articulated teoleostean fishes including *Pachyrhizodus* sp., Ichthyodectoidea, and Clupeoidea with remarkably preserved muscle tissues (Alvarado-Ortega, 2012, pers. obs.).

Small exposures of Palestina-like strata are found within 5 km of the quarry, mostly in road cuts and streambeds where soil is absent. On the basis of recent geological fieldwork in northern Coahuila (SGM, 2008a; 2008b), and comparative analysis of Austin Chalk outcrops in South Texas given by Young and Marks (1952), Paulson (1968), Dravis (1980), Smith (1981), and Young (1985), the Palestina fossiliferous platy beds may be assigned to the lower section of the Austin Chalk (Early Coniacian to Santonian; see additionally Hancock and Walaszczyk, 2004; Myers, 2010). According to Freeman (1961), Lock and Peschier (2006), and Donovan and Staerker (2010), among others, strata equivalent to the Austin Chalk are included as the San Vicente Formation (Boquillas Group) in southwest Texas (Big Bend National Park, Val Verde, Kinney, and Maverick counties; see Figure 1), in the vicinity of the Múzquiz Lagerstätte localities.

Wright (1987) and Young (1985) indicate that sea level rose during deposition of the Austin Chalk, coinciding with the maximum extent of the Cretaceous Interior Seaway, and submerging the large carbonate platforms in northern Mexico and Texas. It has been suggested that deposition of the Austin Chalk may have occurred in water depths of up to 250 m (Young and Marks, 1952)

El Pilote quarry

El Pilote quarry is located 140 km northwest of Múzquiz, at latitude 102°29'51'' W, longitude 28º41'50'' N (Figure 1), within an area mapped as the Eagle Ford Formation (SGM, 2008b). The El Pilote section exposes recrystallized, fossiliferous, marly limestone, interbedded with grayish-brown marl and minor calcareous shale. Distinctive millimeter-scale interstratified non-fissile siltstone layers and iron oxides are also present.

The marly limestone beds contain bivalves, ammonites, and fishes with distinctive fossil preservation. Although fossils occur here sporadically, this locality shares with Palestina quarry a similar style of preservation of the fish specimens. El Pilote fishes include teleosts (Clupeoidea, Pachyrhizodontidae, Ichthyodectiodea, Tselfatiiformes, Enchodontidae, and abundant isolated scales) and teeth of the elasmobranch *Ptychodus* (Alvarado-Ortega *et al.*, 2006).

The El Pilote fossiliferous section has been assigned to upper part of the Eagle Ford Formation (Alvarado-Ortega *et al.*, 2006; Vega *et al.*, 2007; Alvarado-Ortega and Porras-Múzquiz, 2009); the lithology and fossil assemblage here are comparable with those of the Turonian fossiliferous beds exposed at the La Mula and Los Temporales quarries. Nyborg *et al.* (2005) and Stinnesbeck *et al.* (2005) also suggested that the El Pilote outcrops are equivalent to the lower sequence of Upper Turonian strata exposed in the El Rosario quarry. However, more supporting stratigraphic work is required to provide a certain correlation.

Eguiluz de Antuñano (2001) has described limestone, marl, and shale beds about 300 m in thickness belonging to the Eagle Ford Formation that are widespread across several municipalities in northwestern Coahuila, as well as in western, central, and northeastern Texas (Jiang, 1989; and Peschier, 2006, Donovan and Staerker *et al.*, 2010). The Eagle Ford strata were deposited during a time of exceptionally high sea level (Lock *et al.*, 2010). Dawson (1997) and Eguiluz de Antuñano (2001) suggest that these sediments accumulated in a quiet open marine environment in deep waters. Additionally, stratigraphic studies of several members of the Eagle Ford exposed in central Texas show successive transgressive, condensed, and highstand sequences (Freeman, 1961, Donovan and Staerker, 2010, Lock *et al.*, 2010).

Currently, there is a little consensus about the stratigraphic relationships between the quarries where the Múzquiz Lagerstätte are preserved (Blanco-Piñón and Alvarado-Ortega, 2005; Stinnesbeck *et al.*, 2005; Alvarado-Ortega *et al.*; 2006, Vega *et al.*, 2007); the stratigraphy is complicated due to extensive lithofacies variation. These facies changes may have been caused by sea level shifts in the manner shown by Hancock and Walaszczyk (2004). The change from Eagle Ford siliciclastic facies to pelagic chalk of the Austin Chalk is probably a consequence of rising sea level as described by Young (1986) and Goldhammer and Johnson (2001). Thus, the Múzquiz marl-limestone rythmites could be the result of an alternating sedimentary regime within the boundary between the two major facies.

MATERIALS AND METHODS

Samples. Specimens described here are housed in the Museo Histórico de Múzquiz, A. C. (Aguilar and Porras-Múzquiz, 2009), institutional abbreviation MUZ.

The following specimens have been analyzed from the Austin Chalk Formation, Palestina quarry, Acuña Municipality, Coahuila: *Pachyrhizodus* sp. –MUZ 341; clupeid fish – MUZ 602; clupeid fish – MUZ 603; clupeid fish – MUZ 607, *Pachyrhizodus* sp. – MUZ 609, almost complete and articulated specimens showing vertebrate column contracted, digestive tract and muscle mass patches preserved; clupeid fish. – MUZ 596 A and B (part and counterpart), complete and articulated specimen, showing

digestive tract and muscle mass patches preserved.

The following specimens have been analyzed from the Eagle Ford Formation: El Pilote quarry, Múzquiz Municipality, Coahuila: *Pachyrhizodus* sp. – MUZ 73, Head, and trunk part with digestive tract and well-preserved muscle mass patches; clupeid fish – MUZ 602; clupeid Fish – MUZ 325 A and B (part and counterpart), almost complete and articulated specimens showing digestive tract and muscle mass patches preserved.

The soft parts and muscle tissues in the fishes were carefully extracted using surgery needles under a microscope. Subsequently, these were exposed to preliminary cleaning and demineralization with deionized water and, for SEM analysis, partially dissolved using a 5% EDTA carbonate digestive solution (Riquelme *et al.*, 2010). All specimens and samples used for biogeochemical analysis (PIXE and XRD) were not exposed to solvents to avoid contamination or deposition of chemical residues.

Muscle tissue samples: M7 and M7a were extracted from MUZ 596 A and B; M8, M8a and M8b are from MUZ 341; M11, M11a, and M11b were extracted from MUZ 73; M12 and M12b are from MUZ 325 A. Digestive tract samples: M15 was extracted from MUZ 73. Rock samples: M5 is from MUZ 596 A; M6 is from MUZ 341; M9 is from MUZ 607; M10 and M13 are from MUZ 73; M14 is from MUZ 325 A.

UV light. A diagnostic profile of whole specimens was performed using visible fluorescence induced by ultraviolet (UV) light with a range of 254 nm (short wavelength, SW) to 365 nm (long wavelength, LW), and exposure time of less than 3 minutes from 70° to 90° angle of incidence. Microimaging of isolated muscle tissues and sediment samples was acquired with a Edmond E-Zoom 6V video system with EO-3112 Digital CCD camera without any filter. A zoom range of 50X to 480X with oblique/incident UV light was applied for dynamic relief contrast. Corel® Photo-Paint®X 4 software was used for image processing. The biogenic pattern, mineral phases, and hot spots for subsequent chemical analysis were characterized in bones, soft parts, anatomical impressions, as well as in the fossil-bearing rock (Riquelme *et al.*, 2010).

Particle Induced X-ray Emission spectrometry (PIXE). Zones of mineralogical and biological interest, detected in the preliminary study of unprepared fish specimens with UV light, were measured using PIXE based on the external proton beam of 3MeV Tandem Pelletron accelerator of Instituto de Física, UNAM (Ruvalcaba-Sil, 2008). The beam spots were between 1 mm and 0.5 mm in diameter (Riquelme *et al.*, 2009). Light elements were detected using a Si-PIN Amptek detector (150 eV resolution for Mn-Kα line) with a 1 mm diameter Ta collimator, and a Helium jet to improve detection of low energy X rays. Heavier elements were detected using a LEGe detector with a thick Al filter (155µm). The PIXE spectra were collected for 5 minutes and the X-ray detection system was calibrated with pellets of standard reference material from NIST: SRM 2704, SRM 2711, SRM 1880a, SRM 1400, and analytic grade $CaCO_3$ from Sigma Aldrich. The AXIL code and PIXEINT program were used to measure the elemental concentrations expressed as wt% for eight major elements: Al, Si, P, K, Ca, Mn, Fe; and also for nine trace elements at >100 µg/g: S, Ti, Ni, Cu, Zn, As, Sr, Y, U. A review of the PIXE technique is given by Johansson *et al.* (1995).

Scanning Electron Microscopy (SEM). Muscle tissues and fossiliferous rock samples were examined using JEOL JSM-6360 LV and JEOL JSM-5310 scanning electron microscopes. Samples were coated with graphite or gold-palladium and photomicrographs were taken in high vacuum (Riquelme *et al.*, 2010).

X-Ray Diffraction (XRD). Muscle tissues and fossiliferous rock samples were analyzed in air at room temperature using a Bruker AXS™ D8 Advanced equipment with Bragg-Brentano θ-θ geometry, Cu Kα radiation, a Ni 0.5 % Cu- Kβ- filter in the secondary beam and one dimensional position sensitive silicon strip detector (Bruker, Linxeye). The diffraction intensity as a function of the angle 2θ was measured between 20° and 110°, with a 2θ step of 0.01945°, for 53 seconds per point. The crystalline structure, phase composition, and lattice cell parameters of solids were refined with the Rietveld method using the FULLPROF code. Peak profiles were modelled with Pseudo-Voigt functions as shown in Thompson *et al.* (1987), which contained average crystallite size and microstrain as characteristic parameters.

RESULTS

UV light microimaging

Fish body parts including bones, scales, muscle patches, and digestive tracts, are clearly more fluorescent than surrounding sediments under UV light (Figure 3). The Múzquiz fossil-bearing rocks show poor fluorescence in contrast to the enclosed fossils (Figure 3a, 3b). This is mostly observed by a color change associated with flourapatite and calcite as dominant mineral phases in bones, scales, digestive tracts, and muscle tissues. In a clupeid fish (MUZ 596 A and B; Figure 3a, 3b) the color varies under UV light exposure from a saturated white color preliminarily linked to higher phosphorus content in bones; whereas pink, orange, and brown colors are observed in the muscle tissues (Figures 3c, 3d). Additionally, a grayish-white to pale-yellow color is preliminarily linked to calcium-rich bones and scales, whereas bluish, gray, and yellow are observed in the calcium-rich muscle tissues (Figures 3a, 3b). In contrast, dissolved and recrystallized bones and unconsolidated material enriched with siliciclastic minerals are less fluorescent (or notably opaque) under UV light (Figures 3a, 3b).

Although poorly revealed in visible light, the digestive tracts become conspicuous under UV light coupled to microscopy. Results show digestive tracts slightly preserved

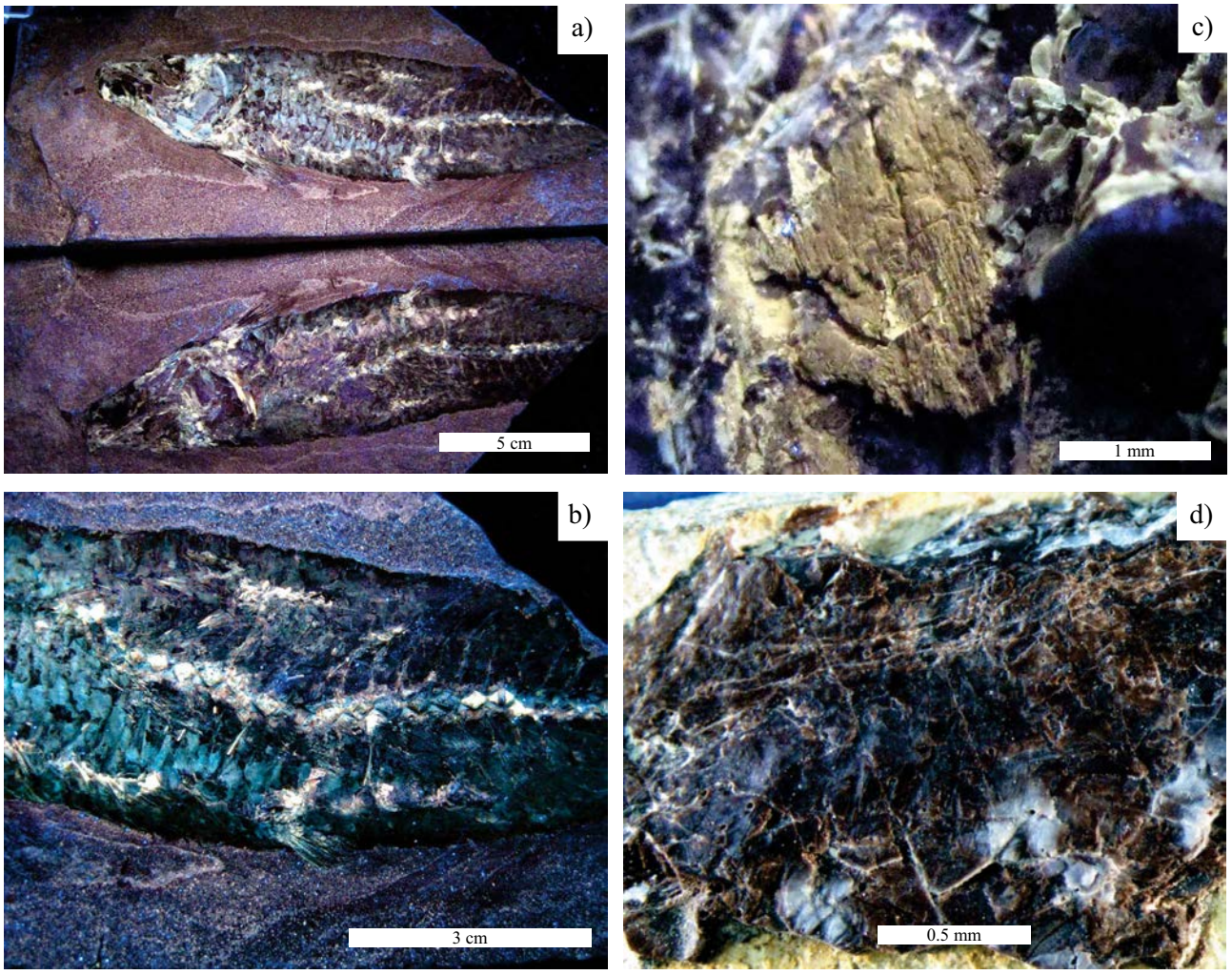

Figure 3. UV light imaging of clupeid fish, (a) part and counterpart (MUZ 596 A and B), Palestina quarry, Austin Chalk, UV light at 365 nm LW; (b) a closer view of same clupeid (MUZ 596 part A), UV light at 254 nm SW; (c) micrograph of trunk muscle tissue near vertebrae of *Pachyrhizodus sp*. (MUZ 73), El Pilote quarry, Eagle Ford Formation, UV light at 254 nm SW (scale bar: 1mm); (d) micrograph of trunk muscle tissue of *Pachyrhizodus sp.* (MUZ 609), Palestina quarry, UV light at 254 nm SW. SW: short wavelength; LW: long wavelength.

(Figure 4), with organic material linked to discernible food remains showing a white, yellow, to brownish color (Figure 4b). The surrounding sediment is less fluorescent, but the thin, more calcareous layers are well defined under UV light (Figure 5). The results show a microstratigraphy of episodic, lime mud layers including shells, calcareous inclusions, and fecal pellets with a white to bluish color (Figures 5b, 5d).

Nondestructive X-ray spectroscopy and mineralogy

On the basis of color variations observed with UV light, certain hot spots were identified for non-destructive PIXE measurements in order to obtain chemical analyses of muscle tissues and sediments avoiding bones and scales. The results of these analyses are summarized in Table 1, and the ratios of diagnostic elements such as P/Ca, Sr/Ca, and S/Ca, may be determined. In the muscle tissues, calcium levels average 21.850 wt%, phosphorus 7.625 wt%, and both strontium (10784 µg/g) and sulfur (2657 µg/g) levels are high (Figures 6, 7). In contrast, the same set of elements in sediments show significantly lower values: calcium levels average 16.924 wt%, and phosphorus 1.552 wt%, whereas the concentrations of some metals increase, such as copper (391 µg/g) and zinc (746 µg/g). This may suggest separate mineralization pathways or incorporation of foreign ions during fossilization. For instance, the average P/Ca ratio of 0.346 in muscle tissue is notably higher than in sediments with 0.092. The average phosphorus concentration in sediment is 1.55 µg/g, but 7.63 µg/g in muscle tissue, an increase in phosphorus content by nearly a factor of five; this is consistent with precipitation and/or recrystallization of phosphate within the primary structure of the muscle tissues.

Bivariate plots of Al/P, Si/P, K/P, Mn/P, and Fe/P indicate differential ion exchange and rearrangement of ele-

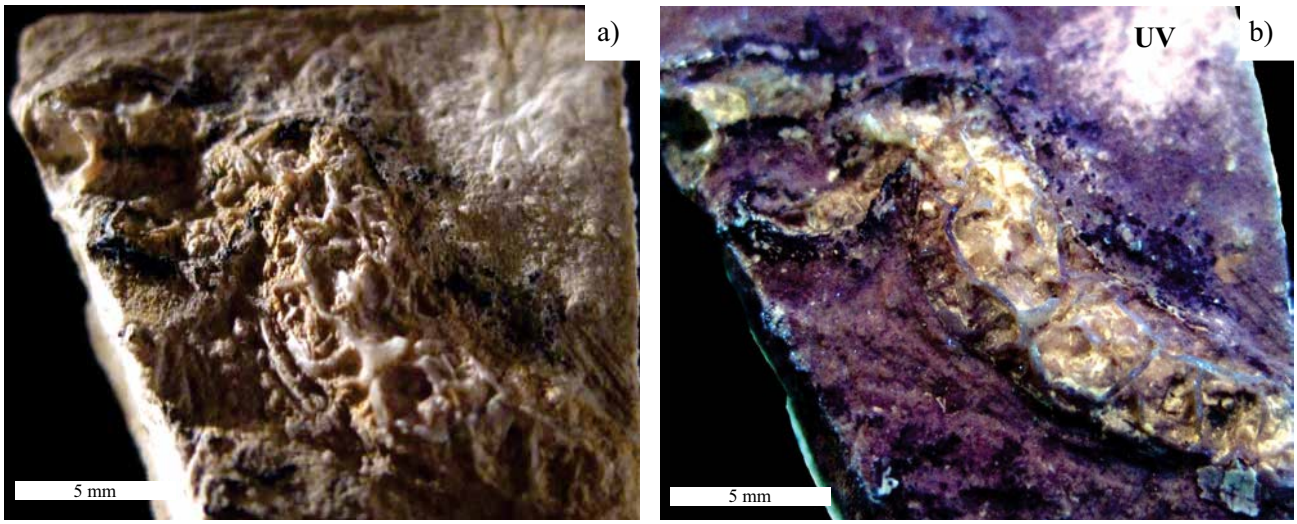

Figure 4. Micrographs of isolated digestive tract of *Pachyrhizodus sp*. (MUZ 73), El Pilote quarry, Eagle Ford Formation. Comparative analysis under regular light (a) and UV light (b) at 365 nm LW.

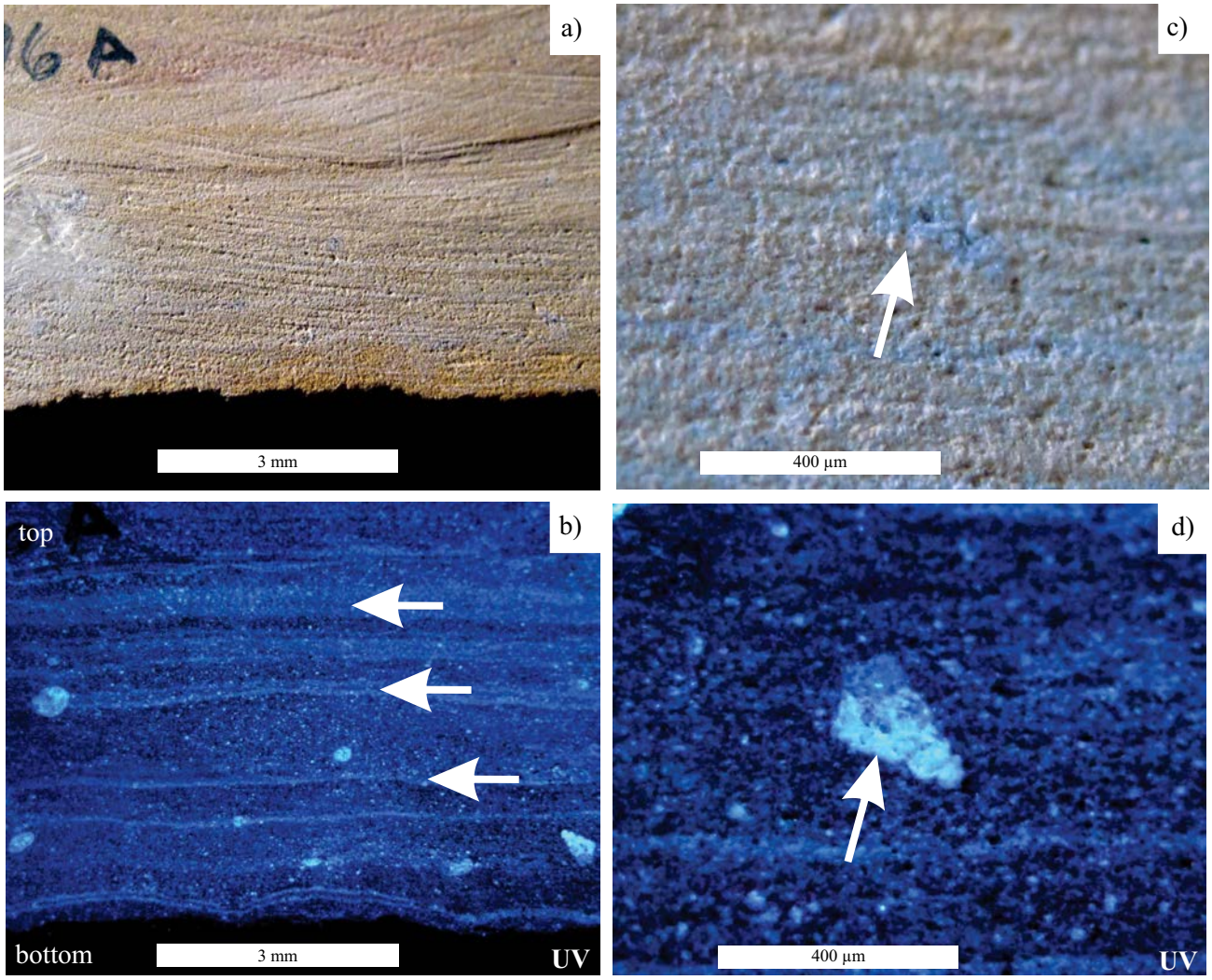

Figure 5. Cross-sectional analysis of the rock containing *Pachyrhizodus sp.* (MUZ 341), Palestina quarry, Austin Chalk. Comparative views under regular light (a) and UV light (b) at 365 nm LW; note the episodic, thin, lime mud layers (arrows) separated by sparry calcite enriched with calcareous fossils (b). Micrographs using regular light (c) and UV light (d); note features that are poorly visible under regular light (c), however, lime mud arrangement and calcareous gastropod shell are clearly visible under UV light (d).

Table1. PIXE multi-elemental analysis. Major element concentrations are expressed in weight percent (wt%) and trace elements in µg/g.

Sample	Spot	Deposit	Al	Si	P	K	Ca	Mn	Fe	S	Ti	Ni	Cu	Zn	As	Sr	Y	U
						wt%								µg/g				
Sediment																		
M5	1	Palestina	0.93	4.29	0.49	1.07	13.34	0.07	0.43	1596	---	501	284	859	14	8192	---	---
	2		2.02	6.78	0.69	1.25	11.65	0.13	0.87	1474	595	1274	530	1915	113	8666	---	---
	3		1.08	4.88	0.60	1.10	13.32	0.04	0.31	1340	---	604	300	1522	---	9752	---	---
M6	1	Palestina	1.59	5.69	0.51	1.21	12.87	0.10	0.41	982	137	213	495	502	---	10010	---	---
	2		1.48	5.50	0.48	1.18	13.21	0.07	0.25	1071	60	439	273	360	---	8798	---	---
	3		0.73	3.07	4.25	0.84	12.69	0.08	0.12	3151	133	198	634	514	---	16098	---	---
M10	1	El Pilote	1.69	16.56	6.05	1.28	26.25	0.03	1.17	1882	857	---	259	706	27	6131	322	---
	2		1.47	20.00	0.35	1.20	21.04	0.02	2.87	1182	---	---	336	473	---	2345	---	---
	3		1.75	23.50	1.74	1.28	27.98	0.10	0.98	1593	---	---	471	101	---	5835	201	---
	4		1.76	14.08	0.38	1.37	16.88	0.02	3.43	1000	---	---	325	504	34	1052	38	---
Muscle tissue																		
M7	1	Palestina	0.96	3.01	3.62	0.89	13.42	0.34	0.60	2830	190	534	268	488	---	12300	---	---
	2		0.80	2.98	3.54	0.98	12.78	0.04	0.29	3320	240	533	256	478	---	9800	---	---
	3		0.89	3.45	4.23	0.87	12.76	0.05	0.24	1780	320	239	239	455	98	8900	97	---
	4		0.99	2.80	4.19	0.96	12.89	0.04	0.32	1780	280	347	298	598	78	10500	---	---
M8	1	Palestina	0.70	2.90	3.78	0.95	12.34	0.06	0.34	1570	340	389	305	673	65	12800	---	---
	2		0.80	2.55	3.58	0.89	12.68	0.06	0.32	1900	290	498	309	887	---	20500	---	---
	3		0.99	2.65	4.21	0.96	12.01	0.06	0.25	2340	320	299	198	498	---	10000	145	---
	4		0.97	2.99	3.89	0.95	13.24	0.04	0.28	3420	410	344	188	587	---	10900	---	---
M11	1	El Pilote	0.87	4.78	13.57	0.18	39.80	0.03	0.36	4428	1103	---	335	657	31	6590	367	---
	2		0.90	9.46	14.74	0.15	38.57	0.03	0.28	2946	---	---	339	51	---	9020	457	---
	3		0.62	1.45	15.81	0.20	40.15	0.02	0.11	2728	---	---	287	441	11	8975	1720	1021
	4		0.38	2.31	16.34	0.15	41.55	0.02	0.11	2844	---	---	388	122	23	9128	1757	1134

ments in carbonates from the fossil-bearing rock (Figure 6). Aluminum, silicon, and potassium are associated with siliciclastic material accumulated during initial deposition of the sediment. In contrast, the manganese and iron content might reflect ionic substitution in secondary minerals precipitated during carbonate diagenesis. According to Boggs (2009), foreign ions such as Mn and Fe are typically concentrated during ion exchange and recrystallization of carbonates as a result of burial diagenetic processes.

Complementary to PIXE analyses, the quantitative XRD results show that flourapatite (FAP) and calcite are the major components in the crystalline phase of muscle tissues (Table 2). Muscle tissues from Palestina quarry exhibit higher concentrations of FAP than of calcite (Figure 8). Although sample M7a from Palestina shows high quartz content, the rest of the samples display lower quartz content, which is linked to post-burial recrystallization. In contrast, muscle tissues from El Pilote show calcite amounts that are higher than that of phosphates. In addition, quartz content is higher in muscle tissues from El Pilote (Figure 8). The quartz content may be related to the quality of fossil preservation; specimens from Palestina show a higher quality of preservation accompanied by minor quartz content and less diagenetic recrystallization.

For both Múzquiz marl and chalky limestone the precursor sediment is composed of a mixture of biogenic carbonates with variable argillaceous material (Table 2). The calcium carbonate content of the fossil-bearing rocks from El Pilote (marly limestone) varies from 90 wt% to 93.90 wt%, whereas rocks from Palestina (chalky limestone) show values ranging from 83.64 wt% to 86.99 wt%. The quartz/calcite ratio (SiO_2/CaO_3) in rocks from Palestina show values ranging from 0.150 to 0.196, whereas rocks from El Pilote show values from 0.065 to 0.110 (Figure 9), suggesting a different input of siliciclastic materials during deposition.

Muscle tissues and microbial biofilms

Electron micrographs show trunk muscle fiber bundles with distinctive fibrillar structure (Figures 10, 11, and 12). Cellular features are preserved, such as highly vascularized areas, and biogenic forms interpreted by their shape, size and location as nucleus-like structures (Figures 10b, 10c), and fragments of sarcoplasmic reticulum that wrap around muscle fibers (Figures 11a, 11b, 11c). The muscle bundles preserved in the Múzquiz fishes are strongly associated with fossil microbes (Figures 11 and 12). A particular network identified among the microbes was interpreted to be organic as they show a spherulitic to spider web-like arrangement, and are linked to the extracellular polymer substance (EPS), which is secreted by microbes as the attachment mechanism in organic or inorganic substrates (Krumbein *et al.*, 2003).

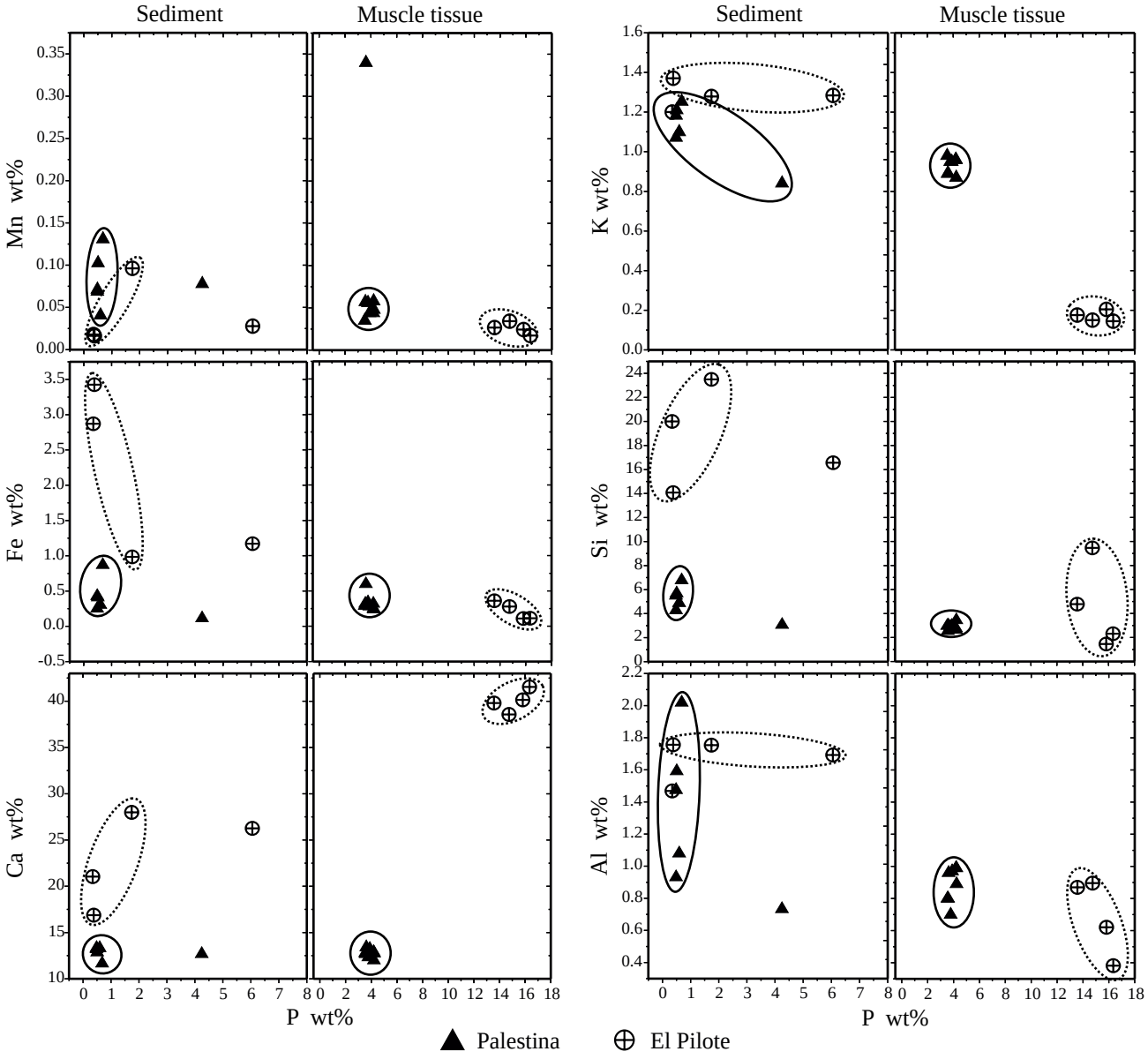

Figure 6. Graphs of element concentrations obtained with PIXE, contrasting muscle tissues and sediments for both Palestina and El Pilote localities. Note the higher concentration of P and Ca in muscle tissues, as well as higher amounts of Al, Si, K, Fe, and Mg in sediments showing differential ion exchange and rearrangement into carbonates that compose the fossil-bearing rocks. Values are expressed in weight percent (wt%); uncertainties are as large as the symbol.

The size and shape of these are consistent with EPS (Figure 11b, 11c).

At higher magnification, bacterial cells are more easily distinguished, and linked to the mineralized EPS surrounding the muscle fibers and sarcoplasmic reticulum (Figure 11). Bacterial cells consist of coccoid (Figures 11b, 11c) and bacilliform morphotypes (Figures 11d, 11f). The spheroidal structure of coccoid cells displays a cryptocrystalline texture on the surface, which is primarily related to cell walls; here tiny crystallites that nucleated around the cell walls are clearly observed (Figure 11c). Micro-fractured crystalline crusts, flakes, and large calcite crystals also occur among the bacilliform bacteria cells (Figure 11d, 11e). Some trunk muscle tissue samples were isolated (Figures 12a, 12b), which show vascular vessels with bacterial spherulitic web-like biofilms within them (Figures 12c, 12d). Complementary evidence of microbial biofilms consists of abundant calcite botryoids in the fossil-bearing rocks (Figure 14c). These crystalline microstructures surrounding the fossils might have formed around bacterial cell-like aggregates.

Cross-sections of the digestive tract show a secondary, continuous growth of crystals that used the organic material as a template. Disordered crystals have developed inside and outside of the biogenic filaments, probably microbial (Figure 13a); whereas capillary aggregates of pseudomor-

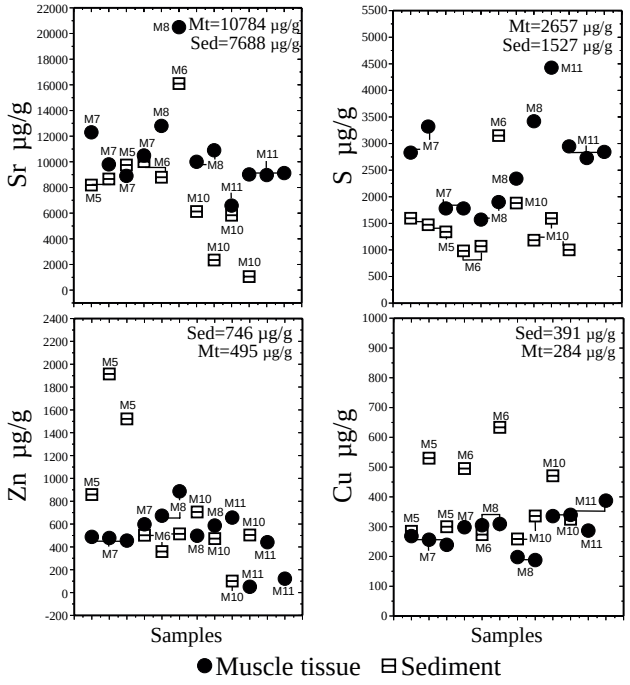

Figure 7. Graphs of element concentration obtained with PIXE, contrasting muscle tissues and sediments, showing higher Sr and S in muscle tissues whereas zinc and copper are lower. Average values for sediment (Sed) and muscle tissue (Mt) are included in each graph. Values are expressed in µg/g and uncertainties are as large as the symbol.

phic carbonates growing alongside the biogenic structures are also observed (Figure 13a, small rectangle). Such crystal growths may be linked to a reducing microenvironment as described by Boggs (2009). There are also significant concentrations of calcareous nanoplankton within the digestive tract (Figures 13b, 13c, 13d). These are also a main component of the associated sediments. However, the calcareous nanoplankton found within the digestive tract show a much higher quality of preservation, including entirely preserved cocospheres (Figure 13d), compared to those within the sediments (Figures 13b, 13c, 14).

Ultrastructural analysis of the fossil-bearing rocks

Although individual beds of the Múzquiz Lagerstätte show great lateral continuity and an apparent monotonous lithology, there are significant differences in the rock composition as seen in their ultrastructural arrangement (Figure 14) and in the microstratigraphy of oriented cross sections (Figure 15). Electron photomicrographs show that coccoliths and elongated calcareous grains in the marly limestone from El Pilote are oriented parallel to the bedding planes (Figure 14a). These rocks have low porosity, and are composed of calcite crystals with a tightly interlocking texture, abundant botroyidal microaggregates, recrystallized and dissolved coccoliths, large calcite flakes, with a pitted microspar fabric (Figure 14a, 14b, 14c).

In contrast, the chalky limestone from Palestina shows a greater diversity of well-preserved coccoliths and less dissolution of the microspar crystals. Also, the microfabric is considerably less interlocking, resulting in increased porosity (Figure 14d, 14e, 14f). These ultra-structures reflect different degrees of diagenetic overprinting, similar to that shown by Munnecke and Westphal (2005), Westphal (2006), and Munnecke *et al.* (2008).

The El Pilote and Palestina rocks also show differences in the size and composition of the micrite grains. The chalky limestone of Palestina shows a fabric composed mostly of calcite crystals larger than 4 µm ('microspar' crystals *sensu* Folk, 1959); as well as a minor content of micrite crystals of ≤ 4 µm size (Figures 14d, 14e). In contrast, the marly limestone from El Pilote shows a significant content of true micrite and only minor microspar crystals (Figures 14a, 14b, 14c). Such crystalline microfabric variability also suggests that the carbonate source is variable, as interpreted in Flügel (2004) and Munnecke *et al.* (2008).

Cross-sectional views of the chalky limestone from Palestina show an upper layer composed of profuse calcareous nanoplankton, calcispheres, and foraminifera, which are cemented with sparry calcite (Figure 15a). This layer (a in Figure 15c) is the horizon where fishes are found in the laminated sediments. The layer below the fish-bearing layer (b in the Figure 15c), has less nanoplankton, calcispheres, and foraminifera cemented with sparry calcite (gray), as well as a very thin argillaceous layer with Fe hydroxides

Table 2. Quantitative X-ray diffraction analysis; values are expressed in weight percent (wt%). FAP: fluoroapatite.

	Sample	FAP	Calcite	Quartz
a. Muscle tissue	*Palestina*			
	M7	94.42	5.58	---
	M7a	78.34	13.73	7.93
	M8	90.30	8.50	1.20
	M8a	93.13	6.97	---
	M8b	82.05	6.97	---
	Pilote			
	M11	61.26	37.65	1.09
	M11a	54.30	43.61	2.09
	M11b	68.10	30.70	1.20
	M12	63.10	35.90	1.00
	M12b	62.25	35.80	1.95

	Sample	Calcite	Quartz	$SiO_2/CaCO_3$
b. Sediment	*Palestina*			
	M5	86.99	13.01	0.150
	M6	83.64	16.36	0.196
	M9	85.20	14.80	0.174
	Pilote			
	M10	90.17	9.83	0.109
	M13	93.90	6.10	0.065
	M14	90.08	9.92	0.110

(reddish; Figure 15b). Such alternating lamination suggests episodic deposition with changes in the sedimentary regime. As shown in Flügel (2004) and Boggs (2009), episodic deposition of calcareous nanoplankton can be consistent with open basin deposition.

DISCUSSION

The fossil fishes from Múzquiz exhibit structural preservation as seen in a "picture frozen in time". The analysis presented here shows that the fossil fishes have a complex mineralogical arrangement in their muscle tissues, which are dominantly preserved by both cryptocrystalline flourapatite (FAP) and semicrystalline calcite in variable concentrations (see PIXE and XRD values, Table 1, Figure 8). Nucleation of phosphate and calcite within the muscle tissues must have occurred simultaneously with organic decay during early burial. Nucleation of FAP and calcite occurring on a small-scale may have caused the immobilization of carcasses and skeletons forming adhesive pellets within and around them in the soft, watery carbonate mud. In soft-bodied fossils, both calcium phosphate and calcite can be present in soft-tissue mineralization as shown by Briggs and Wilby (1996). Accordingly, authigenic mineral crystallization eventually preserves the organic material and may also disrupt organic decay. This implies that for fossil preservation in the marine Múzquiz deposits, the mineralization process may be the critical factor, instead of anoxic or hypersaline conditions, or immediate burial events (which are hard to demonstrate by direct measurements or unambiguous data).

Preserved muscle tissues and digestive tract contents in fossil fishes from a variety of carbonate sediments have been reported previously (*e.g.*, Martill, 1988; Schultze, 1989; Martill, 1990, Maisey, 1991, Wilby and Martill, 1992; Alvarado-Ortega *et al.*, 2007; Trinajstic *et al.*, 2007). There has been some discussion as to whether calcite or apatite is the primary mineral phase involved in the preservation of ancient soft tissues from marine sediments. Maisey (1991, p. 80-88) and Schultze (1989, fig. 21) suggested that muscle tissue in fishes of the Cretaceous Santana Formation of Brazil are preserved in calcite because the tissues disappear with acid preparation, whereas gut contents and those muscles in connection with the digestive tract are truly phosphatized. In contrast, Martill (2012, pers. comm.) suggests that when the muscle tissues are only lightly phosphatized, they fall apart when calcite is removed. As for the apatite, this has long been considered the most significant mineral in soft tissue preservation from marine deposits as shown for example by Martill (1988), Allison and Briggs (1991), Lucas and Prèvôt (1991), Briggs *et al.* (1993), and Martill (2003).

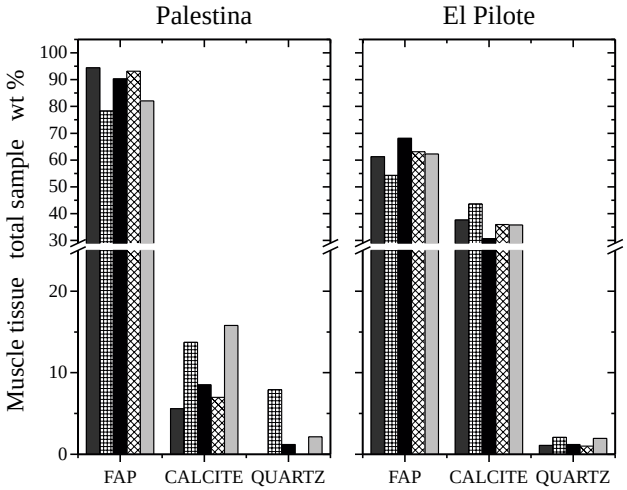

Figure 8. Graph of X-ray diffraction results for muscle tissues. Note the higher content of flourapatite (FAP) in samples from Palestina quarry, whereas calcite is significantly higher in samples from El Pilote.

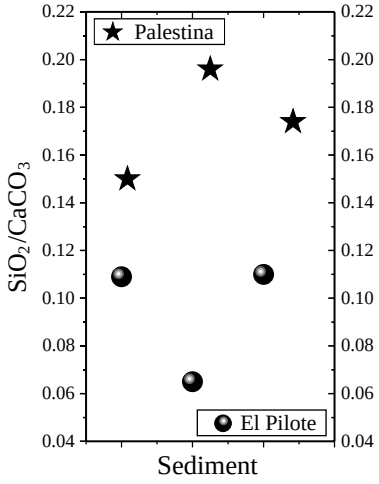

Figure 9. Graph of $SiO_2/CaCO_3$ ratio in sediments obtained from XRD analysis.Differences in $SiO_2/CaCO_3$ ratio (quartz/calcite) as shown for the Palestina and El Pilote localities suggest significant variations during depositional input.

The physicochemical mechanism for soft tissue preservation in marine deposits is also not fully understood. Martill (1989) proposed the "Medusa Effect", which is a rapid lithification process. It seems that this can be possible only at a small-scale and organ level; however, the actual petrification mechanism remains unexplained. This hypothesis is similar to the cellular permineralization theory presented by Schopf (1975). Although challenged by Maisey (1991), the Medusa Effect is typically based on phosphatization process (Martill, 1988; Martill, 2003).

According to Briggs (2003a), the quality of preservation induced by authigenic phosphatization is primarily linked to crystallinity: the size and arrangement of phosphate-based crystallites, as well as to the sediment input. Briggs (2003b) suggests that preservation of muscle tissues requires the replication of their morphology by rapid *in situ* growth of minerals, *i.e.*, authigenic mineralization, which depends on several factors including the nature of microbial activity, organic decay gradients, availability of ions, and the

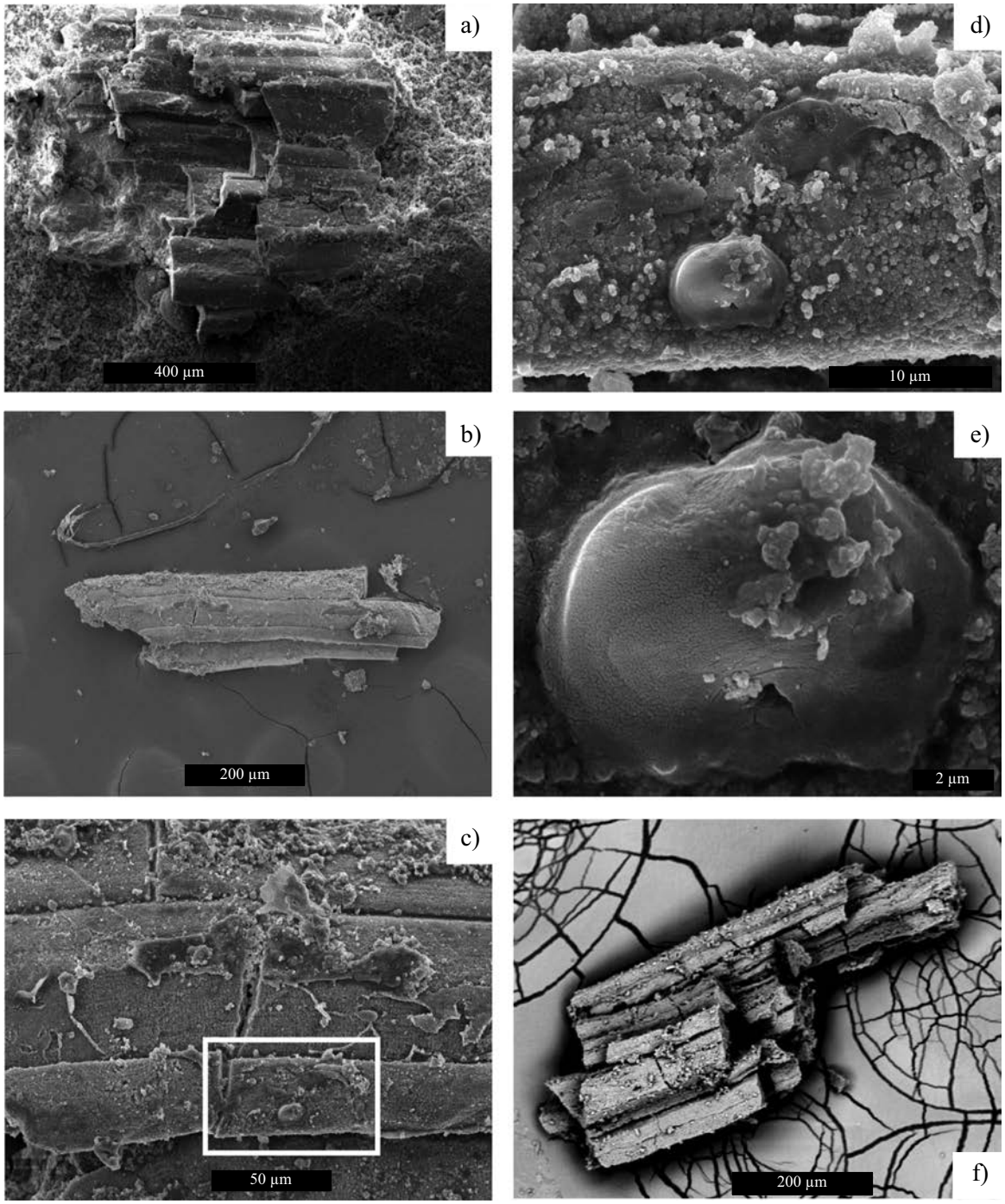

Figure 10. Electron micrographs of (a) muscle tissue extracted from *Pachyrhizodus sp.* (MUZ 73), El Pilote quarry, Eagle Ford Formation; (b) isolated thick muscle fibers of the previous sample after partial carbonate dissolution by EDTA; (c - e) closer views of same muscle fibers showing biogenic form interpreted by shape, size, and location as nucleus-like structure; (f) muscle tissue extracted from clupeid fish MUZ 596 A.

biology of the organisms that are fossilized. Additionally, Dornbos (2010) considered that selective phosphatization is controlled by a microbial environment at limited depths on the seafloor, with bacterial cells operating as phosphate nucleation points. It is generally accepted that such chemical and structural transformation in a short period of time (hours or days) implies rapid mineralization, which can interrupt organic decay (Martill, 1988; Allison and Briggs, 1991; Lucas and Prèvôt, 1991; Briggs *et al.*, 1993; Martill, 2003; Dornbos, 2010), rather than a long-term fossilization mechanism governed by predominantly sedimentary processes, as in the classical concepts of preservational modes (Schopf, 1975).

Mineralization of cells and subcellular structures oc-

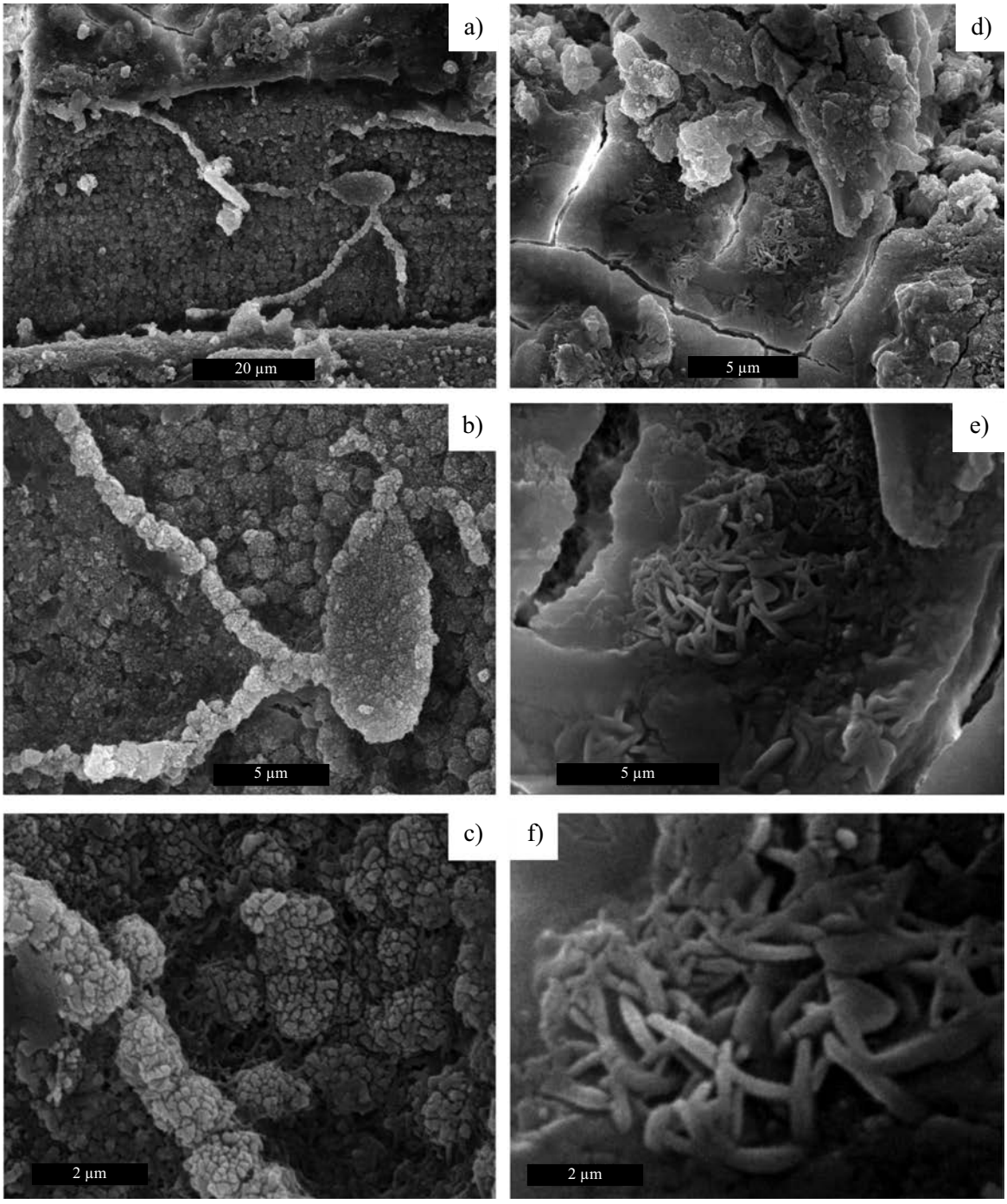

Figure 11. Muscle tissue of *Pachyrhizodus sp.* (MUZ 73), El Pilote quarry, Eagle Ford Formation. Electron micrographs of (a - c) biogenic form interpreted by shape, size and location as sarcoplasmic reticulum remain; (c) microbial biofilm showing characteristic arrangement of spherulitic to spider-web-like form; (d - f) bacilliform bacteria in same muscle tissue surrounded by thick calcite flakes.

curs at a molecular level, induced by spontaneous chemical reactions in supersaturated solutions (Weiner and Dove, 2003; Qiu and Orme, 2008; Weiner and Addadi, 2011). As documented by De Yoreo and Vekilov (2003), Weiner and Dove (2003), and Weiner and Addadi (2011), the onset of this process occurs as a mineral nucleation spot (crystal 'embryo' or crystal 'seed'), is followed by intense crystal growth (secondary nucleation) using the organic material as a template (see Figure 11). Depending on the chemical composition of the biomolecules and the reactive mineral solution involved, this mineralized organic template may gain or lose fidelity compared with the original morphotype (Mann, 2001).

Accordingly, it seems that the detail-rich preserva-

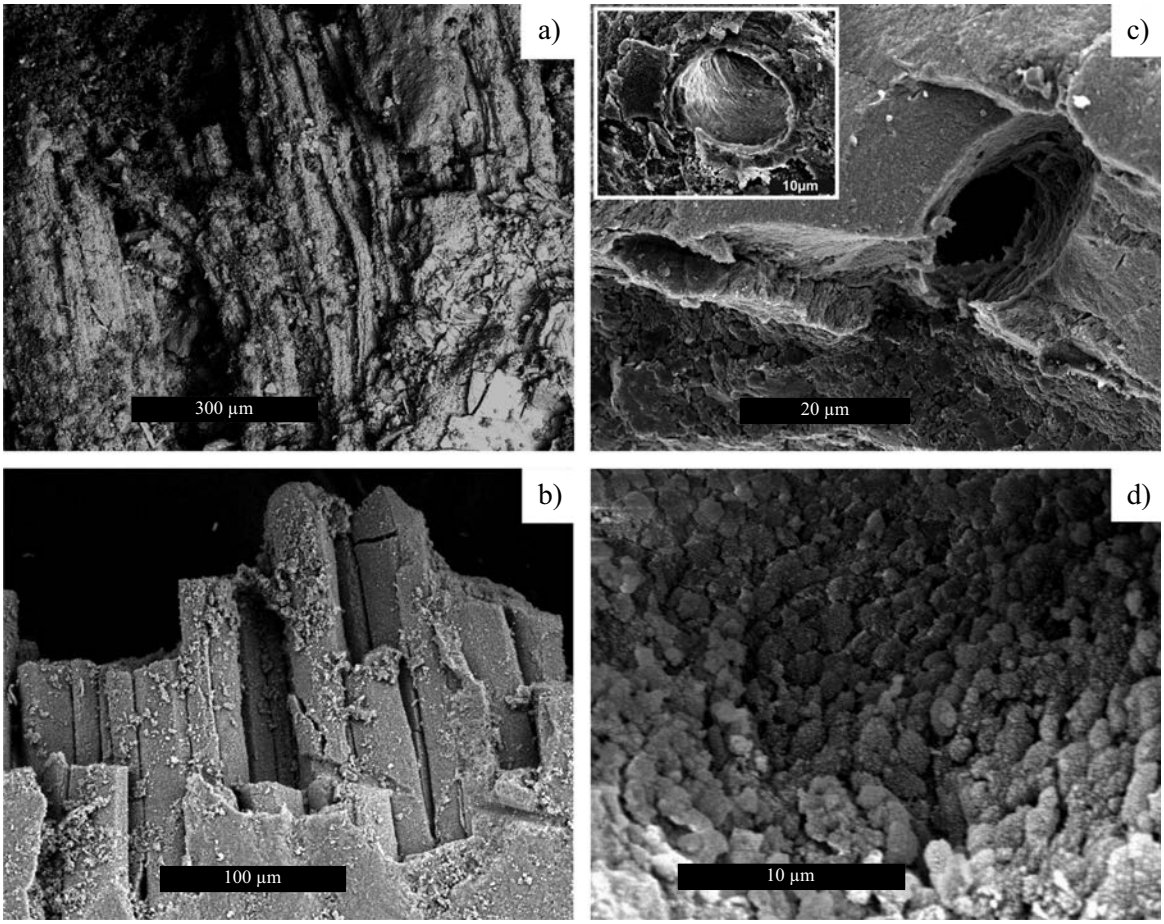

Figure 12. Electron micrographs of (a) muscle tissue from clupeid fish (MUZ 596 A), Palestina quarry, Austin Chalk; (b) muscle tissue from *Pachyrhizodus sp.* (MUZ 609); (c) vascular vessels observed in same muscle tissues (small rectangle scale bar = 10 µm); (d) bacterial biofilm with spherulitic web-like form within it.

tion of muscle tissues at Múzquiz occurred as a result of mineral nucleation and subsequent crystal growth at a macromolecular level. The crystal growth here may have been a consequence of natural occurring dissolved calcium phosphate and semicrystalline carbonate in the seafloor microenvironment; and the seawater is the saline solution that acted as the crystallization precipitant factor. Increased temperature during early burial may also accelerate mineralization. Mineral precipitation in this supersaturated system may induce the crystal growth in cells and rapid biomineralization of soft tissues, biofilms, and microbes (see additionally Frankel and Bazylinskn, 2003).

The "crystal seed" process presented above is probably the mineralization pathway that explains soft tissue preservation at the cellular and subcellular level. The physicochemical dynamics of the crystal seed process are largely known and thoroughly investigated in biomineralization research as shown by Mann (2001), De Yoreo and Vekilov (2003), Weiner and Dove (2003), and Weiner and Addadi (2011), among others.

Another critical aspect of the present work concerns the microbial preservation. Fossil soft tissues represent an important source of microbial fossilization. Biofilms associated with fossil soft tissues in vertebrates and invertebrates from marine Lagerstätten have been reported elsewhere (Wilby *et al.*, 1996; Toporski *et al.*, 2002; Krumbein *et al.*, 2003; Liebig, 2003; Briggs *et al.*, 2005, among others). According to Sanderman and Amundson (2003), and Briggs *et al.* (2005), the occurrence of biofilms within soft tissues is strongly associated with an assemblage of heterotrophic microorganisms that degrade carcasses. Microbes interact with their environment through surface reactions and metabolic activities (Gall, 2003; Krumbein *et al.*, 2003). It is likely that microbial growth on carcasses generates a closed environment that fixes P and Ca cations (Visscher and Stolz, 2005); this is known as bacterial sealing (Krumbein *et al.*, 2003). The interaction of microbes and minerals can generate a sequence of biogeochemical reactions that facilitate biomineralization of organic matter during burial in deposits such as those observed in the fossiliferous Múzquiz beds (Gall, 2003; Flügel, 2004, Westphal, 2006; Munnecke *et al.*, 2008). Eventually degrading microbes drive mineralization on themselves through fixing P and Ca cations on their cell walls (Frankel and

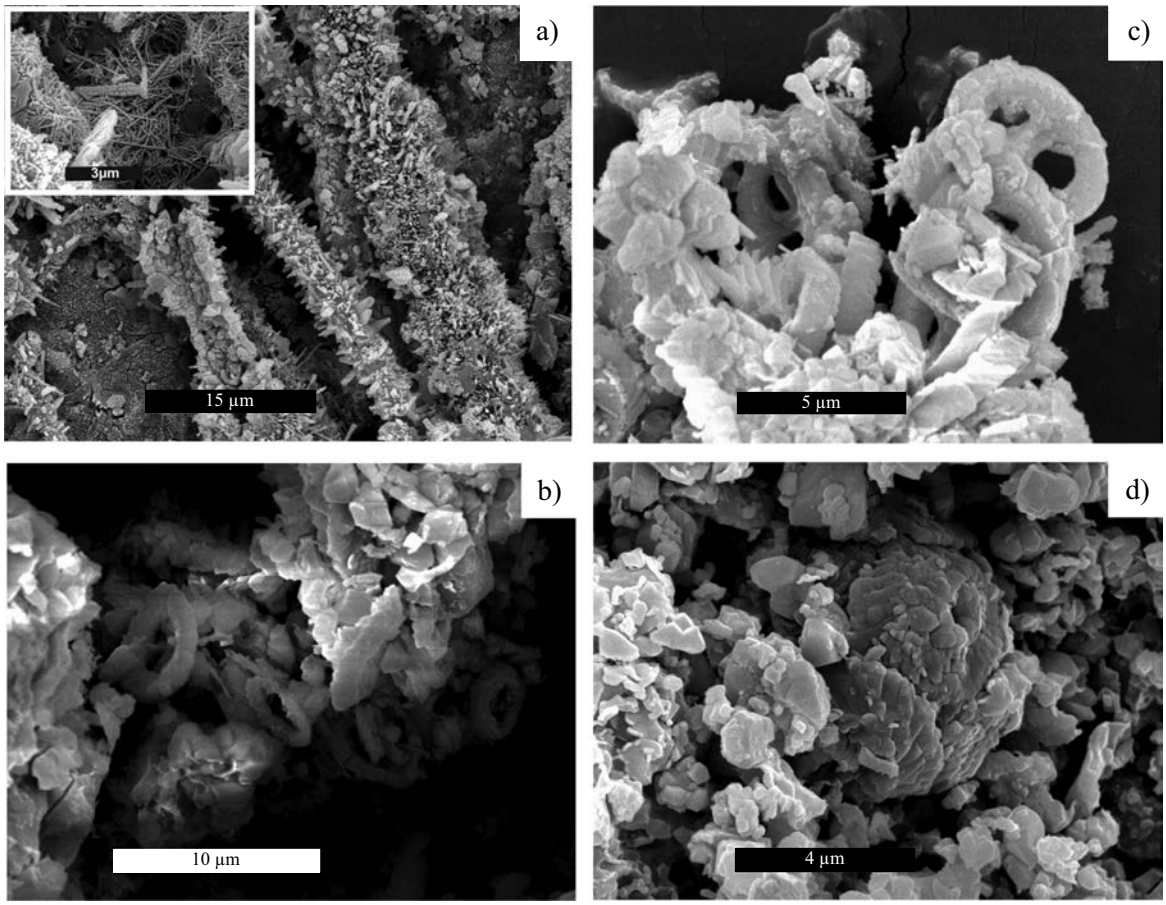

Figure 13. Electron micrographs of digestive tract contents as observed in *Pachyrhizodus sp.* (MUZ 341), Palestina quarry, Austin Chalk. (a) Disordered crystals growing inside and outside of biogenic filaments, likely microbial, as well as capillary aggregates of pseudomorphic carbonates growing alongside same filaments (small rectangle scale bar 3 µm); (b - c) well-preserved coccoliths and enclosed calcareous fragments linked to the chalky sediments; (d) intact cocosphere surrounded by coccolith fragments as preserved within digestive tract.

Bazylinskn, 2003; Krumbein *et al.*, 2003; Liebig, 2003).

Finally, the source and mobilization of dissolved phosphate and semicrystalline carbonate in the Múzquiz Lagerstätte is linked to the decaying organisms and microbial mats. As shown by Allison and Briggs (1991), Briggs *et al.* (1993), Dornbos (2010), a significant source of dissolved P and Ca cations in marine burials is released from decaying carcasses, whereas microbial metabolism is implicated in their mobilization through the water column (Krumbein *et al.*, 2003). Fish biology might also contribute as intrinsic factor that increases their preservation potential. Schultze (1989), Martill (1990), Maisey (1991), and Wilby and Martill (1992) have suggested that dietary intake can be a natural source of limiting elements such as phosphorus. Shewfelt (1981) demonstrated that muscle tissues and soft parts of extant fishes show high concentrations of available Ca and P cations as micro-bioelements related to dietary habits.

The availability of Ca, P, S, and Na cations, and CO_2 molecules, associated with biomineralization of soft tissues in marine burials is critical. As described by Lucas and Prèvôt (1991), Sanderman and Amundson (2003), and Boggs (2009), an important source comes from carbonate precipitation that formed the seafloor sediments. Emerson and Bender (1981) also report that another significant source of Ca, P, Na cations and CO_2 molecules may be calcareous nanoplankton deposited on the seafloor. This is consistent with the episodic deposition of calcareous nanoplankton observed in the Múzquiz sediments (Figures 14, 15).

CONCLUSIONS

Examination of fossils under UV light has previously been undertaken with vertebrates from Lagerstätten sediments preserved elsewhere (Tischlinger and Frey, 2002; Hone *et al.*, 2010, Kellner *et al.*, 2010; among others). Such analyses have focused on detailed morphological examination of the specimens as preserved on the bedding plane in the fossiliferous rock. In the present work, UV-light microscopy was supplemented with PIXE as a useful tool to extract biogeochemical information from exceptionally preserved fossils. This typically non-destructive technique

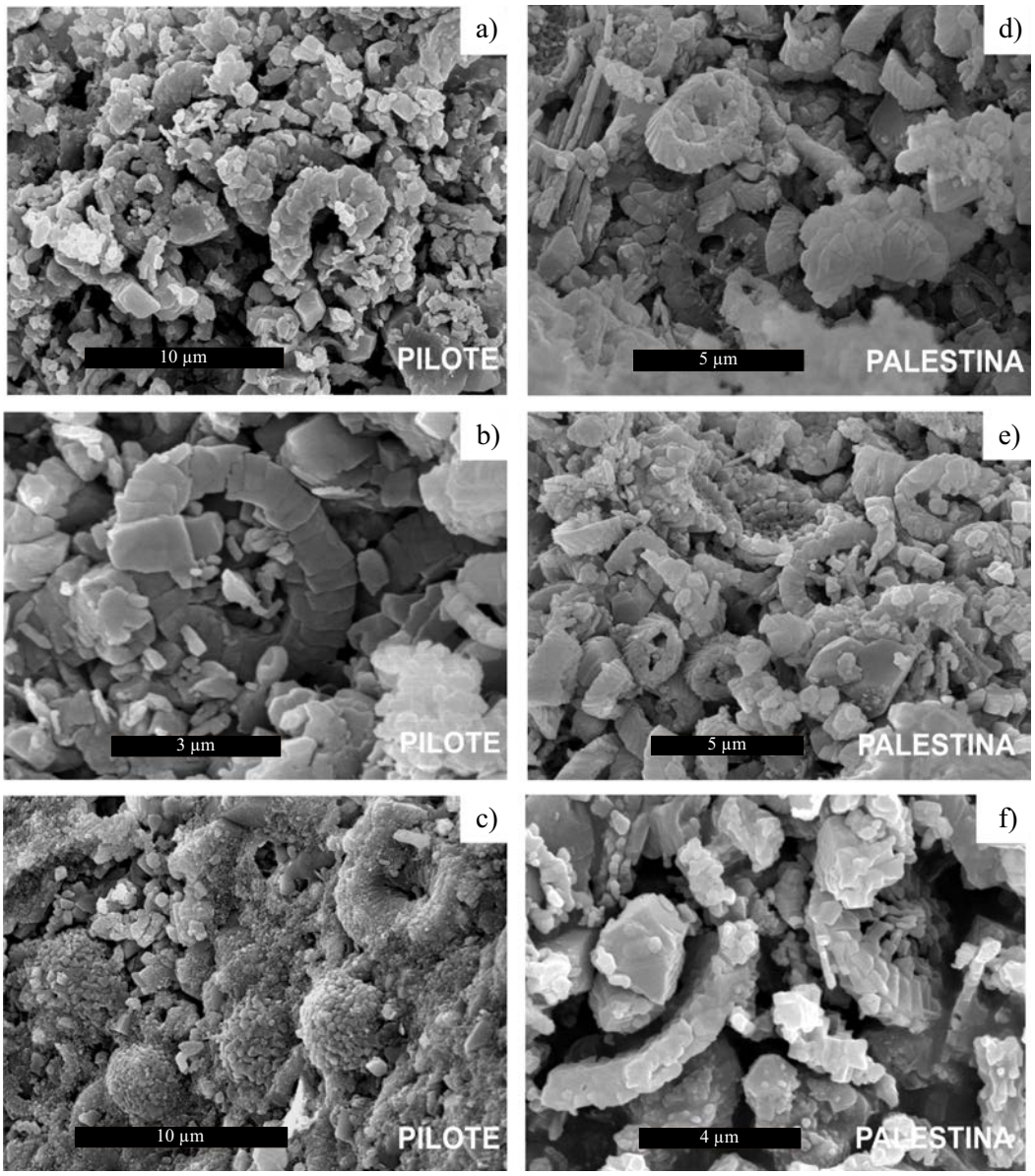

Figure 14. Ultrastructural analysis of rocks contrasting the El Pilote locality (left) and Palestina locality (right); (a) poorly preserved coccoliths and dissolved calcareous debris oriented parallel to the bedding planes; (b) tightly interlocking texture and microspar fabric; (c) botryoidal microaggregates of calcite crystallites, dissolved coccoliths, carbonate flakes, and pitted microspar; (b - d) Palestina sediments in contrast show less interlocking microspar crystals, well-preserved coccoliths, and less dissolution.

can be carried out on unprepared samples without causing any damage or alteration to the fossil material or matrix (Riquelme *et al.*, 2009).

Accordingly, results have shown different major and trace element abundances for the matrix sediment and muscle tissues of the fossil fishes. These chemical signatures may serve as diagnostic fingerprints that allow for interpretation of the fossil preservation process. The "crystal seed" process discussed here is a coherent theory that may explain the physicochemical reactions that occurred during rapid mineralization of ancient soft tissues. This might also apply to non-carbonate or non-phosphate composites including sulfates, silicates, iron oxides, and others authigenic minerals.

ACKNOWLEDGEMENTS

This work is part of the postgraduate-granting program of Biological Sciences at the UNAM, financially supported by CONACYT. The authors thank Karim López and Francisco Jaimes for technical support during experimental runs at the Pelletron, IF-UNAM. Special thanks for SEM imaging and analysis go to Yolanda Hornelas from

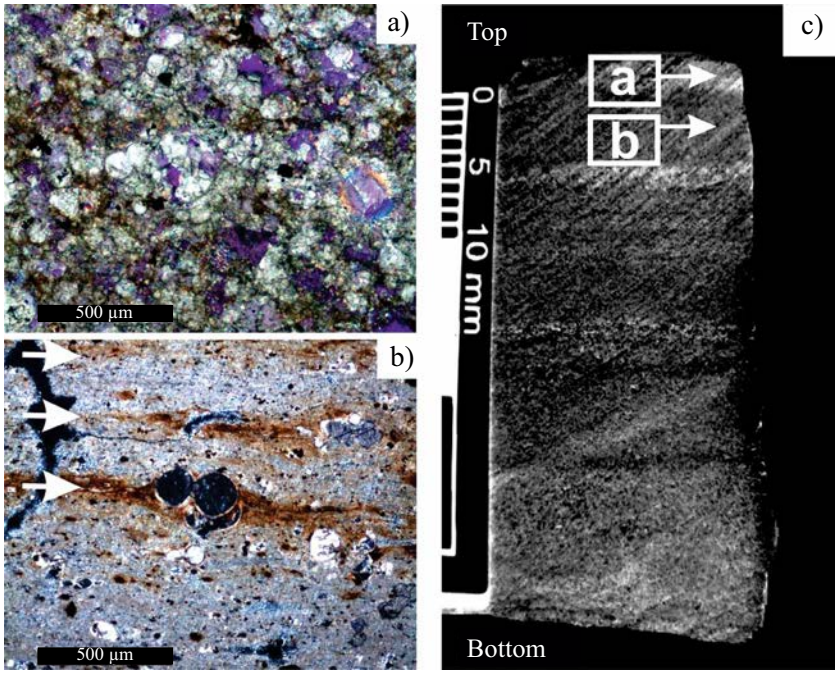

Figure 15. Thin-sections of Palestina quarry sediment showing (a) profuse well-preserved calcareous nanoplankton, calcispheres, and foraminifera; this represents the zone where the fossil fishes occur; (b) layer below fish-bearing horizon showing notably less nanoplankton, calcispheres, and poor foraminiferal remains cemented with sparry calcite (gray), as well as thin, reddish argillaceous layers shown by arrows; (c) fossil-bearing rock, a thinly laminated chalky limestone; the letters a and b represent the position of the previous thin sections.

ICMYL-UNAM, Silvia Espinosa FC-UNAM, and Jaqueline Cañetas IF-UNAM. We would also like to thank people from the limestones quarries in Múzquiz and Acuña area for help in fossil collection: Juan Manuel Santos, Juan Quintana, Tania Aguirre, Maestra Esperanza, El Pilo, and El Diablo. Also thanks to Drs. David Martill, Joseph Peterson, and Thomas Lehman for valuable comments that improved the manuscript. This research has also been partially supported by PAPIIT-UNAM grants IN403210 and IN225008, as well as CONACYT endowment U49839-R.

REFERENCES

Aguilar, F., Porras-Múzquiz, H., 2009, Los fósiles del Museo de Múzquiz A. C. y su resguardo patrimonial por el Instituto Nacional de Antropología e Historia: Boletín de la Sociedad Geológica Mexicana, 61(2), 147-153.

Allison, P.A, Briggs D.E.G., 1991, Taphonomy of nonmineralized tissues, *in* Allison, P.A., Briggs, D.E.G. (eds.), Taphonomy, Releasing the Data Locked in the Fossil Record: New York, Plenum Press, 26-58.

Allison, P.A., 1988, Konservat-Lagerstätten: cause and classification: Paleobiology, 14(4), 331-344.

Alvarado-Ortega, J., Porras-Múzquiz, H., 2009, On the occurrence of *Gillicus arcuatus* (Cope, 1875) (Pisces, Ichthyodectiformes) in Mexico: Boletín de la Sociedad Geológica Mexicana, 61(2), 215-224.

Alvarado-Ortega, J., Blanco-Piñón, A., Porras-Múzquiz, H., 2006, Primer registro de *Saurodon* (Teleostei: Ichthyodectiformes) en la cantera La Mula, Grupo Eagle Ford (Cretácico Superior: Turoniano), Múzquiz, Estado de Coahuila, México: Revista Mexicana de Ciencias Geológicas, 23(1), 107-112.

Alvarado-Ortega, J., Espinosa-Arrubarrena, L., Blanco-Piñón, A., Vega, F., Benammi, M., Briggs, D.E.G., 2007, Exceptional preservation of soft tissues in Cretaceous fishes from the Tlayúa Quarry, Central Mexico: Palaios, 22, 682-685.

Blanco-Piñón, A., Alvarado-Ortega, J., 2005, Fishes from La Mula quarries, a new Late Cretaceous locality from the vicinity of Múzquiz, Coahuila, NE Mexico, *in* Poyato-Ariza , F.J. (ed.), Extended Abstracts, Fourth Internacional Meeting on Mesozoic Fishes –Systematics, Homology, and Nomenclature, Miraflores de la Sierra, Madrid, August 8–14: Madrid, Spain, Universidad Autónoma de Madrid, UAM Ediciones, 37-41.

Boggs, S., 2009, Petrology of sedimentary rocks: New York, Cambridge University Press, 311-526.

Botjer, D.J., Etter, W., Hagadorn, J.W., Tang, C.M., 2002, Fossil-Lagerstäten: jewels of the fossil record, *in* Botjer D.J., Etter W., Hagadorn J.W., Tang C.M. (eds.), Exceptional fossil preservation, a unique view of the ervolution of marine life: New York, Columbia University Press, 1-10.

Briggs, D.E.G., 2003a, Exceptionally preserved fossils, *in* Briggs, D.E.G., Cowther, P.R. (eds.), Palaeobiology II: Malden, USA, Blackwell Publishing, 328-332.

Briggs, D.E.G., 2003b, The role of decay and mineralization in the preservation of soft bodied fossils, Annual Review of Earth and Planetary Sciences, 31, 275-301.

Briggs, D.E.G., Wilby, P. R., 1996, The role of the calcium carbonate/calcium phosphate switch in the mineralization of soft-bodied fossils: Journal of Geological Society of London, 153, 665-668.

Briggs, D.E.G., Kear, A.J., Martill, D.M., Wilby, P.R., 1993, Phosphatization of soft-tissue in experiments and fossils: Journal of the Geological Society, 150(6), 1035-1038.

Briggs, D.E.G., Moore, R.A., Shultz, J.W., Schweigert, G., 2005, Mineralization of soft-part anatomy and invading microbes in the horseshoe crab *Mesolimulus* from the Upper Jurassic Lagerstätte of Nusplingen, Germany: Proceedings of the Royal Society B, 272, 627-632.

Buchy, M.C., Smith, K.T., Frey, E., Stinnesbeck, W., González-González, A.H., Ifrim, C., López-Oliva, J.G., Porras-Muzquiz, H., 2005, Annotated catalogue of marine squamates (Reptilia) from the Upper Cretaceous of northeastern Mexico: Netherlands Journal of Geosciences – Geologie en Mijnbouw, 84(3), 195-205.

Dawson, W.C., 1997, Limestone microfacies and sequence stratigraphy: Eagle Ford Group (Cenomanian-Turonian) North-Central Texas outcrops: Gulf Coast Association of Geological Societies Transactions, 47, 99-105.

De Yoreo, J.J., Vekilov, P.G., 2003, Principles of crystal nucleation and growth, *in* Dove, P.M., De Yoreo, J.J., Weiner, S. (eds.), Biomineralization: Mineralogical Society of America, Reviews in Mineralogy and Geochemistry, 54, 57-94.

Donovan, A.D., Staerker, T.S., 2010, Sequence stratigraphy of the Eagle Ford (Boquillas) Formation in the subsurface of South Texas and outcrops of West Texas: Gulf Coast Association of Geological Societies Transactions, 60, 861-899.

Dornbos, S.Q., 2010, Phosphatization trough the Phanerozoic, *in* Allison, P.A., Bottjer, D.J. (eds.), Taphonomy: Process and Bias through Time: New York, Springer, Topics in Geobiology Book Series, 32, 435-453.

Dravis, J.J., 1980, Sedimentology and diagenesis of the Upper Cretaceous Austin Chalk Formation. South Texas and Northern Mexico: Texas, Rice University, PhD Thesis, 513 p.

Eguiluz de Antuñano, S., 2001, Geologic evolution and gas resources of the Sabinas Basin in Northeastern Mexico, *in* Bartolini, C., Buffler , R.T., Cantú-Chapa, A. (eds.), The western Gulf of Mexico Basin: Tectonics, sedimentary basins, and petroleum systems: American Association of Petroleum Geologists, Memoir 75, 241-270.

Emerson, S., Bender, M., 1981, Carbon fluxes at the sediment-water interface of the deep-sea: calcium carbonate preservation: Journal of Marine Research, 39, 139-162.

Flügel, E., 2004, Microfacies data: matrix and grains, *in* Microfacies of carbonate rocks. Analysis, interpretation and application: Berlin, Springer-Verlag, 73-176.

Folk, R.L., 1959: Practical petrographical classification of limestones: American Association of Petroleum Geologists Bulletin, 43, 1-38.

Frankel R.B., Bazylinskn, D. A., 2003, Biologically induced mineralization by bacteria, *in* Dove, P.M., De Yoreo, J.J., Weiner, S. (eds.), Biomineralization: Mineralogical Society of America, Reviews in Mineralogy and Geochemistry, 54, 57-94.

Freeman, V. L., 1961, Contact of Boquillas flags and Austin Chalk in Val Verde and Terrell Counties, Texas: American Association of Petroleum Geologists Bulletin, 45(1),105-107.

Frey, E., Buchy, M.C., Stinnesbeck, S., González-González, A., Di Stefano, A., 2006, *Muzquizopteryx coahuilensis* n.g., n. sp., a nyctosaurid pterosaur with soft tissue preservation from the Coniacian (Late Cretaceous) of northeast Mexico (Coahuila): Oryctos, 6, 47-66.

Gall, J.C., 2003, Role of microbial mats, *in* Briggs, D.E.G., Cowther, P.R. (eds.), Palaeobiology II: Malden, USA, Blackwell Publishing, 280-284.

Goldhammer, R.K., 1999, Mesozoic sequence stratigraphy and paleogeographic evolution of northeast Mexico, *in* Bartolini, C., Wilson, J.L., Lawton T.F. (eds.), Mesozoic sedimentary and Tectonic History of North-Central Mexico: Boulder, Colorado, Geological Society of America Special Paper 340, 1-58.

Goldhammer, R.K., Johnson, C.A., 2001, Middle Jurassic-Upper Cretaceous paleogeographic evolution and sequence-stratigraphic framework of the northwest Gulf of Mexico rim: American Association of Petroleum Geologists, Memoir 75, 45-81.

Hancock, J.M., Walaszczyk, I., 2004, Mid-Turonian to Coniacian changes of sea level around Dallas, Texas*:* Cretaceous Research, 25, 459-471.

Hone, D.W.E., Tischlinger H., Xu, X., Zhang, F., 2010, The extent of preserved feathers on the four-winged dinosaur *Microraptor gui* under Ultraviolet Light: Plos One, 5 (2), 9223.

Jiang, M.J., 1989, Biostratigraphy and geochronology of the Eagle Ford Shale, Austin Chalk and lower Taylor Marl in Texas based on calcareous nannofossils: College Station, Texas A&M University, PhD Thesis, 524 p.

Johansson, S.A.E., Campbell, J.L., Malmqvist, K.G., 1995, Particle-induced X-ray emission spectrometry (PIXE), *in* Widefrodner J.D. (ed), Chemical Analysis: New York, John Wiley & Sons, Series of monographs on analytical chemistry and its applications, v. 133, 451 p.

Kellner, A.W.A., Wang, X., Tischlinger, H., de Almeida Campos, D., Hone, D.W.E., Meng, X., 2010, The soft tissue of *Jeholopterus* (Pterosauria, Anurognathidae, Batrachognathinae) and the structure of the pterosaur wing membrane: Proceedings of the Royal Society B 227, 321-329.

Krumbein,W.E., Brehm, U., Gerdes, G., Gorbushina, A.A., Levit, G., Palinski, K.A., 2003, Biofilm, biodictyon, biomat microbialites, oolites, stromatolites, geophysiology, global mechanism, parahistology, *in* Krumbein, W.E., Paterson, D.M. , Zarvarzin, G.A. (eds.), Fossil and recent biofilms: a natural history of life on Earth: Dordrecht, Kluwer Academic Publishers, 1-27.

Larson, P.A., Morin, R.W., Kauffman, E.G., Larson, A., 1991, Sequence stratigraphy and cyclicity of lower Austin/upper Eagle Ford outcrops (Turonian-Coniacian), Dallas County, Texas: Dallas Geological Society, Field Trip Guidebook #9, 61 p.

Liebig, K., 2003, Bacteria, *in* Briggs, D.E.G., Cowther, P.R. (eds.), Palaeobiology II: Malden, USA, Blackwell Publishing, 253-256.

Lock, B.E., Peschier, L., 2006, Boquillas (Eagle Ford) upper slope sediments, West Texas: outcrop analogs for potential shale reservoirs: Gulf Coast Association of Geological Societies Transactions, 56, 491-508.

Lock, B.E., Peschier, L., Whitcomb, N., 2010, The Eagle Ford (Boquillas Formation) of Val Verde County, Texas -a window on the South Texas play: Gulf Coast Association of Geological Societies Transactions, 60, 419-434.

Lucas, J., Prèvôt, L.E., 1991, Phosphates and Fossil Preservation, *in* Allison, P.A., Briggs, D.E.G. (eds.), Taphonomy, Releasing the Data Locked in the Fossil Record: New York, Plenum Press, 389-405.

Maisey, J.G., 1991, Santana Fossils: An Illustrated Atlas: New York, T.F.H. Publications, 459.

Mann, S., 2001, Biomineralization, principles and concepts in bioinorganic materials chemistry: Oxford, U.K, Oxford University Press, 193 p.

Martill, D.M., 1988, Preservation of fish in the Cretaceous Santana Formation of Brazil: Palaeontology, 31, 1-18.

Martill, D.M., 1989, The Medusa effect: Instantaneous fossilization: Geology Today, 5, 201-205.

Martill, D.M., 1990, Macromolecular resolution of fossilized muscle tissue from an elopomorph fish: Nature, 346, 171-172.

Martill, D.M., 2003, The Santana Formation, *in* Briggs, D.E.G., Cowther, P.R. (eds.), Palaeobiology II: Malden, USA, Blackwell Publishing, 351-356.

Munnecke, A., Westphal, H., 2005, Variations in primary aragonite, calcite, and clay in fine-grained calcareous rhythmites of Cambrian to Jurassic age – an environmental archive?: Facies, 51, 611-626.

Munnecke, A., Westphal, H., Kölbl-Ebert, M., 2008, Diagenesis of plattenkalk: examples from the Solnhofen area (Upper Jurassic, southern Germany): Sedimentology 55, 1931-1946.

Myers, T., 2010, Earliest occurrence of the Pteranodontidae (Archosauria: Pterosauria) in North America: New material from the Austin Group of Texas: Journal of Vertebrate Paleontology, 84(6), 1071-1081.

Nyborg, T., Alvarado-Ortega, J., Blanco, A., Vega, F.J., 2005, Taphonomy of fish preserved within ammonite chambers from the Upper Cretaceous Austin Group, Coahuila, Mexico: Geological Society of America Abstracts with Programs, 37(7), 159 p.

Paulson, O.L., 1968, Correlations in Austin group of Texas: American Association of Petroleum Geologists Bulletin, 52(5), 864-866.

Qiu, S.R., Orme, C.A., 2008, Dynamics of biomineral formation at the near-molecular level: Chemical Reviews, 108, 4784-4822.

Riquelme, F., Ruvalcaba-Sil, J.L., Alvarado-Ortega, J., 2009, Palaeometry: non-destructive analysis of fossil materials: Boletín de la Sociedad Geológica Mexicana, 61(2), 177-183.

Riquelme, F., Alvarado Ortega, J., Ruvalcaba Sil, J.L., Hornelas-Orozco, Y., Espinoza-Matías, S., Linares-López, C., Aguilar-Franco, M., 2010, Microanálisis ultraestructural y multielemental en la fosilización selectiva de localidades Lagerstätten del Cretácico Tardío (Turoniano) en Coahuila, México, *in* X Congreso Nacional de Microscopía, Extended Abstracts, Morelia, Mich., 23-27 may: México, Asociación Mexicana de Microscopía, A.C., 3 p.

Ruvalcaba-Sil, J.L., 2008, Las técnicas de origen nuclear: PIXE y RBS, *in* Del Egido, M.A., Calderón, T. (eds.), La Ciencia y el Arte: Madrid, Instituto del Patrimonio Histórico Español (IPHE)-CSIC, 151-172.

Sanderman, J., Amundson, R., 2003, Biogeochemistry of decomposition and detrital processing, *in* Holland, H.D., Turekian, K.K. (eds.), Treatise on Geochemistry: Oxford, Elsevier Pergamon, v. 8, Biogeochemistry, 249-316.

Schopf, J.M., 1975, Modes of fossil preservation: Review of Palaeobotany and Palynology, 20, 27-53.

Schultze, H.P., 1989, Three-dimensional muscle preservation in Jurassic fishes of Chile: Revista Geológica de Chile, 16(2), 183-215.

Seilacher, A., Reif, W.E., Westphal, F., Riding, R., Clarkson, E.N.K., Whittington, H.B., 1985, Sedimentological, ecological and temporal patterns of fossil lagerstätten (and discussion): Philosophical Transactions of the Royal Society B, 311 (1148), 5-24.

SGM (Servicio Geológico Mexicano), 2008a, Carta Geológica–Minera Ciudad Acuña H14-7, escala 1:250,000: Servicio Geológico Mexicano, 1 map.

SGM (Servicio Geológico Mexicano), 2008b, Carta Geológica–Minera San Miguel H13-12, escala 1: 250,000: Servicio Geológico Mexicano, 1map.

Shewfelt, R.L., 1981, Fish muscle lipolysis –A review: Journal of Food Biochemistry, 5, 79-100.

Smith, C.C., 1981, Calcareous nannoplankton and stratigraphy of late Turonian, Coniacian, and early Santonian age of the Eagle Ford and Austin Groups of Texas: United States Geological Survey ,Professional Paper 1075, 98 p.

Sohl, N.F., Martinez, R.E., Salmerón-Ureña, P., Soto-Jaramillo, F., 1991, Upper Cretaceous, *in* Salvador, A. (ed.), The Gulf of Mexico Basin: Boulder, Colorado, Geological Society of America, Decade of North American Geology, The Geology of North America, v. J, 205–244.

Stinnesbeck, W., Ifrim, C., Schmidt, H., Rindfleisch, A., Buchy, M.C., Frey, E., González-González, A.H., Vega, F.J., Cavin, L., Keller, G., Smith, K.T., 2005, A new lithographic limestone deposit in the Upper Cretaceous Austin Group at El Rosario, county of Múzquiz, Coahuila, northeastern Mexico: Revista Mexicana de Ciencias Geológicas, 22(3), 401-418.

Thompson, P., Cox, D.E., Hasting, J.B., 1987, Rietveld refinement of Debye-Scherrer synchrotron X-ray data from Al_2O_3: Journal of Applied Crystallography, 20, 79.

Tischlinger, H., Frey, E., 2002, Ein *Rhamphorhynchus* (Pterosauria, Reptilia) mit ungewöhnlicher Flughauterhaltung aus dem Solnhofener Plattenkalk: Archaeopteryx, 20, 1-20.

Toporski, J.K.W., Steele, A., Westall, F., Avci, R., Martill, D.M., McKay, D.S., 2002, Morphologic and spectral investigation of exceptionally well-preserved bacterial biofilms from the Oligocene Enspel formation, Germany: Geochimica et Cosmochimica Acta, 66, 1773-1791.

Trinajstic, K., Marshall, C., Long, J., Bifield, K., 2007, Exceptional preservation of nerve and muscle tissues in Late Devonian placoderm fish and their evolutionary implications: Biology Letters, 3, 197-200.

Vega, F.J., Nyborg, T., Rojas-Briceño, A., Patarroyo, P., Luque, J., Porras-Múzquiz, H., Stinnesbeck, W., 2007, Upper Cretaceous Crustacea from Mexico and Colombia: similar faunas and environments during Turonian times: Revista Mexicana de Ciencias Geológicas, 24 (3), 403-422.

Visscher, P.T., Stolz, J.F., 2005, Microbial mats as bioreactors: populations, processes and products: Palaeogeography, Palaeoclimatology, Palaeoecology, 219, 87-100.

Weiner, S., Dove, P.M., 2003, An overview of biomineralization processes and the problem of the vital effect, *in* Dove, P.M., De Yoreo, J.J., Weiner, S. (eds.), Biomineralization: Mineralogical Society of America, Reviews in Mineralogy and Geochemistry, 54, 1-29.

Weiner, S., Addadi, L., 2011, Crystallization pathways in biomineralization: Annual Review of Materials Research, 41, 21-40.

Westphal, H., 2006, Limestone–marl alternations as environmental archives and the role of early diagenesis: a critical review: International Journal of Earth Sciences – Geologische Rundschau, 95, 947-961.

Wilby, P.R., Martill, D.M., 1992, Fossil fish stomachs: A microenvironment for exceptional preservation: Historical Biology, 6, 25-36.

Wilby, P.R., Briggs, D.E.G., Bernier, P., Gaillard, C., 1996, Role of microbial mats in the fossilization of soft tissues: Geology, 24, 787-790.

Wright, E.K., 1987, Stratification and paleocirculation of the Late Cretaceous Western Interior Seaway of North America: Geological Society of America Bulletin, 99, 4, 480-490.

Young, K., 1985, The Austin division of central Texas, *in* Woodruff, C.M. (ed.), Austin Chalk in its Type Area; Stratigraphy and Structure: Austin, Texas, Austin Geological Society Guidebook, 7, 3-52.

Young, K., 1986, Cretaceous, marine inundations of the San Marcos Platform, Texas: Cretaceous Research, 7, 117-140.

Young, K., Marks, E., 1952, Zonation of Upper Cretaceous Austin Chalk and Burditt Marl, Williamson County, Texas: American Association of Petroleum Geologists Bulletin, 36(3), 477-488.

Manuscript received: September 29, 2012
Corrected manuscript received: November 25, 2012
Manuscript accepted: November 30, 2012